JOURNAL OF AGRICULTURAL AND FOOD CHEMISTRY

pubs.acs.org/JAFC Article

XBP1s-Regulated GFPT1 via Facilitating O-GlcNAcylation of FASN S509 Is Involved in Arsenic-Induced MASLD through Promoting Fatty Acid Synthesis in Hepatocytes

Wenjie Li,[#] Bowen Fan,[#] Han Li,[#] Qiong Du,[#] Jiaheng Lin, Yi Yang, Xiaolin Ding, Haoran Zhang, Haibo Xia, Binafsha Manzoor Syed, Cheng Cheng,[*] and Qizhan Liu[*]

Cite This: https://doi.org/10.1021/acs.jafc.6c00603 Read Online

ACCESS | Metrics & More | Article Recommendations | Supporting Information

ABSTRACT: Arsenic in groundwater and agricultural systems poses a challenge to food safety and public health. Although environmental arsenic exposure is a risk factor for metabolic dysfunction-associated steatotic liver disease (MASLD), its molecular mechanism remains unclear. Chronic arsenic exposure induced hepatic steatosis and upregulated fatty acid synthase (FASN) in mice. Mechanistically, arsenic triggered splicing of X-box binding protein 1 (XBP1) into its active form, XBP1s, which promoted the transcription of glutamine-fructose-6-phosphate aminotransferase 1 (GFPT1). This increased flux of the hexosamine biosynthetic pathway (HBP) elevated UDP-GlcNAc and O-GlcNAcylation. Mass spectrometry identified Ser509 as an O-GlcNAcylated site on FASN, and its mutation abolished arsenic-induced lipid accumulation. O-GlcNAcylation at Ser509 stabilized FASN by inhibiting ubiquitin-mediated degradation and promoting fatty acid synthesis. This study identifies the XBP1s-GFPT1 axis and O-GlcNAcylation of FASN S509 as essential in arsenic-induced MASLD.

KEYWORDS: *metabolic dysfunction-associated steatotic liver disease, arsenic, O-GlcNAcylation, X-box binding protein 1*

1. INTRODUCTION

Arsenic is a widely distributed environmental contaminant whose exposure constitutes a public health concern worldwide. It currently endangers more than 50 million individuals in at least 22 countries and regions.[1] Despite the 10 μg/L standard established by the United States Environmental Protection Agency (EPA) and World Health Organization (WHO) in 2016, arsenic levels in groundwater throughout Cambodia, Bangladesh, Uruguay, India, and China continue to exceed this limit.[2] Human exposure to arsenic occurs chiefly through contaminated drinking water and food, which becomes contaminated during agricultural production.[3] Arsenic enters the food chain in this process primarily through crop absorption from soil and water, as well as through human practices such as pesticide use.[4] Chronic arsenic exposure causes damage to various organs and systems, including skin lesions; neurodevelopmental dysfunctions; and a greater susceptibility to liver, lung, and bladder cancers.[5] Recent evidence indicates that arsenic exposure is linked to metabolic diseases, including diabetes, atherosclerosis, and metabolic syndrome.[6] These health effects impose heavy economic and social burdens on global public health systems; thus, it is urgent to elucidate the mechanisms underlying chronic arsenic toxicity.

Metabolic dysfunction-associated steatotic liver disease (MASLD) is a chronic metabolic liver disorder with a feature of hepatocellular lipid accumulation; it affects approximately 30% of adults worldwide. As an early stage in the liver disease spectrum, it may progress to fibrosis, cirrhosis, and hepatocellular carcinoma if not effectively treated.[7] Apart from genetic, dietary, and lifestyle determinants, environmental pollutant exposure is recognized as a risk factor for MASLD.[8] As the primary organ for arsenic metabolism, the liver is consequently a key target for its toxicity and is highly sensitive to exposure.[9] Arsenic exposure triggers liver injury via mechanisms such as oxidative stress, mitochondrial dysfunction, endoplasmic reticulum (ER) stress, and epigenetic alterations.[10,11] Our previous work confirmed that arsenic exposure induces steatohepatitis, hepatic fibrosis, and hepatocellular carcinoma.[12−14] Current evidence suggests that intervening in hepatic steatosis during its initial phases to halt its development may prevent adverse outcomes such as cirrhosis and hepatic carcinoma at a relatively low cost.[15] Therefore, the present study focused on the initial stage of liver injury, which is hepatic lipid accumulation.

O-Linked N-acetylglucosamine modification (O-GlcNAcylation) is a dynamic and reversible post-translational process that adds N-acetylglucosamine to serine or threonine residues. It modulates the activity and stability of various proteins, including transcription factors, metabolic enzymes, and signaling proteins, thereby contributing to processes such as cellular energy metabolism, stress response, and gene expression.[16] The only substrate donor for O-GlcNAcylation is uridine diphosphate N-acetylglucosamine (UDP-GlcNAc). The synthesis of UDP-

Received: January 12, 2026
Revised: March 19, 2026
Accepted: March 24, 2026

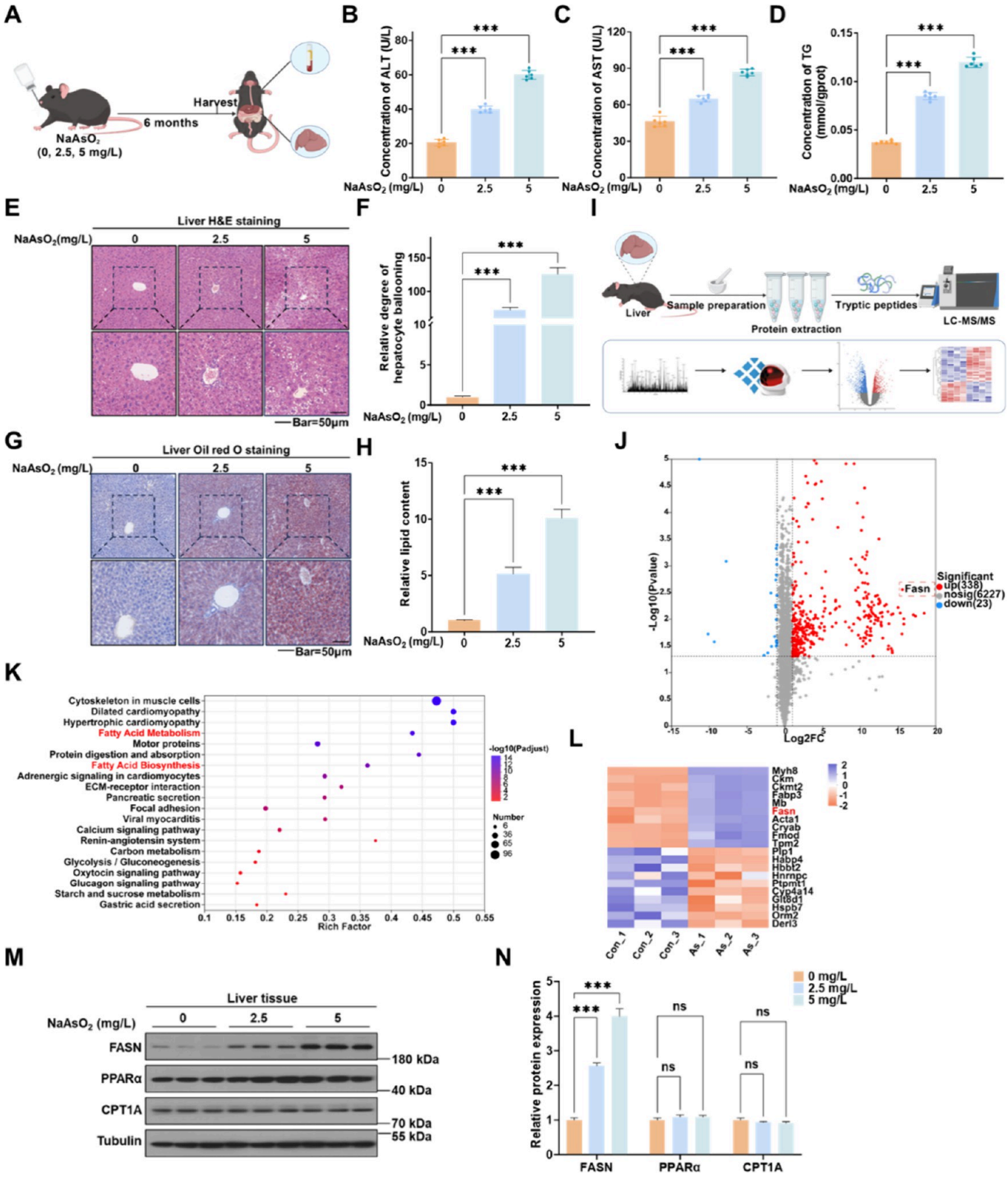

Figure 1. Chronic arsenic exposure disrupts fatty acid metabolism of livers and induces MASLD in mice. C57BL/6J mice were supplied with drinking water containing 0, 2.5, or 5 mg/L $NaAsO_2$ for 6 months. (A) Schematic diagram of arsenic exposure of mice. The serum levels of ALT (B) and AST (C), and the hepatic levels of TG (D) were measured in mice ($n = 6$). (E) Representative H&E-stained liver sections (scale bar = 50 μm) and (F) the corresponding quantification of hepatocyte ballooning ($n = 6$). (G) Representative Oil Red O-stained liver sections (scale bar = 50 μm) and (H) the corresponding quantification of relative lipid content ($n = 6$). (I) Schematic diagram of the mouse liver proteomics analysis. (J) Volcano plot of proteins identified by quantitative proteomics in the arsenic group versus controls ($n = 3$). (K) KEGG pathway enrichment analysis for significantly changed proteins upon arsenic treatment ($n = 3$). (L) Heatmap of the top 20 differentially expressed proteins from the arsenic versus control comparison ($n = 3$). (M) Western blots were prepared, and (N) relative protein levels of FASN, PPARα, and CPT1A in the liver were quantified ($n = 6$).

https://doi.org/10.1021/acs.jafc.6c00603
J. Agric. Food Chem. XXXX, XXX, XXX−XXX

GlcNAc depends on the hexosamine biosynthetic pathway (HBP), a branch of glucose metabolism. In this pathway, glutamine-fructose-6-phosphate amidotransferase 1 (GFPT1) acts as the rate-limiting enzyme to catalyze the production of UDP-GlcNAc.[17] The maintenance of metabolic homeostasis is dependent on O-GlcNAcylation, which link it to the pathogenesis of numerous metabolic diseases.[18−20] The imbalance of O-GlcNAcylation in MASLD contributes to disease pathogenesis, potentially acting as a pathogenic driver by disrupting hepatic lipid metabolism, insulin signaling, and inflammatory responses.[20−22] Emerging evidence suggests a role for O-GlcNAcylation in arsenic-induced MASLD, although the mechanisms require further elucidation.

During ER stress, inositol-requiring enzyme 1α (IRE1α) is activated and catalyzes unconventional splicing of X-box binding protein 1 (XBP1) mRNA, producing the transcription factor XBP1s to regulate diverse target genes.[23] XBP1s is a regulator in various pathological processes, including tumor proliferation, inflammatory bowel disease, and Alzheimer's disease.[24−26] XBP1s promotes lipid accumulation in hepatocytes and drives MASH-related inflammation and fibrosis in macrophages via the NLRP3 and TGF-β pathways.[27] XBP1s levels correlate with MASLD severity, highlighting its promise as a disease progression biomarker and as a pharmacological target.[28] However, the involvement of XBP1s in arsenic-induced MASLD remains unexplored and requires exploration.

The present study sought to clarify the impact of O-GlcNAcylation on the development of an arsenic-induced MASLD. With mice, we characterized via proteomics the hepatic protein landscape following chronic arsenic exposure. The mechanistic basis for the observed changes was elucidated by using HepG2 cells and primary mouse hepatocytes. Combining transcription factor binding site prediction with chromatin immunoprecipitation (ChIP) assays, we established that O-GlcNAcylation is regulated by XBP1s via GFPT1, which controls the flux of HBP. Moreover, co-immunoprecipitation (Co-IP) and mass spectrometry (MS) assays confirmed that site-specific O-GlcNAcylation of fatty acid synthase (FASN) stabilizes the protein and promotes fatty acid synthesis. Steatosis in hepatic organoids was attenuated upon the inhibition of XBP1s. These findings reveal the involvement of the XBP1s-GFPT1-FASN signaling axis in regulating arsenic-induced MASLD and provide new insights for targeted therapeutic strategies.

2. MATERIALS AND METHODS

2.1. Experimental Animals and Housing Conditions

Male C57BL/6J mice (6−8 weeks old) were purchased from the Experimental Animal Center of Nanjing Medical University. The animals were housed in a specific pathogen-free (SPF) barrier facility with the following environmental conditions: temperature at 22−26 °C, relative humidity 30−70%, 12 h/12 h light−dark cycle, regular ventilation, and ambient noise below 40 dB. Body weights were monitored weekly. All animal experimental procedures were conducted in strict accordance with international guidelines for animal care and use. All efforts were made to minimize animal suffering by using anesthesia and analgesics during potentially painful procedures. The animal study protocol was approved by the Animal Welfare Ethics Committee of Nanjing Medical University (IACUC-2409057).

2.2. Mouse Models

A chronic arsenic-exposure model was established by administering sodium arsenite ($NaAsO_2$; Sigma, 99.0%) in the drinking water to C57BL/6J mice on a standard diet for 6 months. The mice were randomly divided into three groups (n = 6) that received 0, 2.5, or 5 mg/L $NaAsO_2$. The doses were selected based on body surface area conversion from average arsenic levels in contaminated groundwater (450 μg/L) to the human equivalent dose.[29] The selection also considered the higher arsenic metabolic rate in mice, with supporting evidence from hepatic arsenic data.[30]

In the 6-diazo-5-oxo-L-norleucine (DON) intervention model, C57BL/6J mice were randomly assigned to the control, arsenic exposure (5 mg/L $NaAsO_2$), or arsenic + DON groups (n = 6). Mice in the intervention group were cotreated with arsenic and DON, which were administered via intraperitoneal injection at 1 mg/kg (MedChemExpress, USA; 99.9%) once weekly for 12 weeks. The DON dose was derived from a previous report.[31]

In the toyocamycin intervention model, C57BL/6J mice were randomly divided into four groups (n = 6), comprising the control, arsenic exposure (5 mg/L $NaAsO_2$), toyocamycin intervention, and DMSO vehicle control groups. Mice in the intervention group were co-treated with arsenic and toyocamycin, an adenosine analog and an antibiotic, which was administered via intraperitoneal injection at 0.5 mg/kg (MedChemExpress, USA; 99.9%) once weekly for 12 weeks. The DMSO vehicle control group was treated with the solvent alone. The toyocamycin dose was selected on the basis of previous studies.[32]

2.3. Statistical Analysis

Statistical analyses were performed using GraphPad Prism 10.1.2 and IBM SPSS Statistics 21.0. Data are presented as means ± standard deviation (SD). The normality of data distribution was assessed using the Shapiro−Wilk test. For data conforming to a normal distribution, an unpaired two-tailed Student's t test was used for comparisons between two groups, and analysis of variance (ANOVA) followed by Tukey's post hoc test was used for comparisons among three or more groups. All experiments were independently repeated at least three times. Values of $p < 0.05$ were considered statistically significant, with significance levels indicated in figures as ns (not significant), $^*p < 0.05$, $^{**}p < 0.01$, or $^{***}p < 0.001$.

For brevity, methodological details not elaborated here are available as part of the Supporting Information.

3. RESULTS

3.1. Chronic Arsenic Exposure Disrupts Fatty Acid Metabolism of Livers and Induces MASLD in Mice

To model chronic exposure, C57BL/6J mice were maintained on drinking water containing 0, 2.5, or 5 mg/L $NaAsO_2$ for 6 months (Figure 1A). Although an increasing trend was evident, the rise in the liver-to-body weight ratios induced by arsenic exposure did not reach statistical significance (Figure S1A). However, exposure elevated serum aminotransferase levels (ALT and AST), indicating impaired liver function (Figure 1B,C). Hepatic triglyceride (TG) levels were also elevated in arsenic-exposed mice (Figure 1D). H&E staining revealed that arsenic exposure disrupted hepatic architecture, with hepatocytes exhibiting extensive vacuolation (Figure 1E,F). Oil Red O and BODIPY staining revealed hepatic steatosis in arsenic-exposed mice (Figure 1G,H and Figure S1B), confirming that arsenic exposure induced lipid accumulation.

Following proteomic sequencing of liver tissues (Figure 1I), principal component analysis revealed a distinct separation between the arsenic-treated and control groups (Figure S1C). Screening for differentially expressed proteins revealed 361 candidates, with 338 being upregulated and 23 downregulated (Figure 1J). KEGG enrichment analysis showed that arsenic exposure altered pathways related to fatty acid metabolism and fatty acid synthesis (Figure 1K), with a notable increase in the level of FASN (Figure 1L). Further validation experiments confirmed that although the expression of PPARα and CPT1A remained largely unchanged, arsenic exposure led to an

https://doi.org/10.1021/acs.jafc.6c00603
J. Agric. Food Chem. XXXX, XXX, XXX−XXX

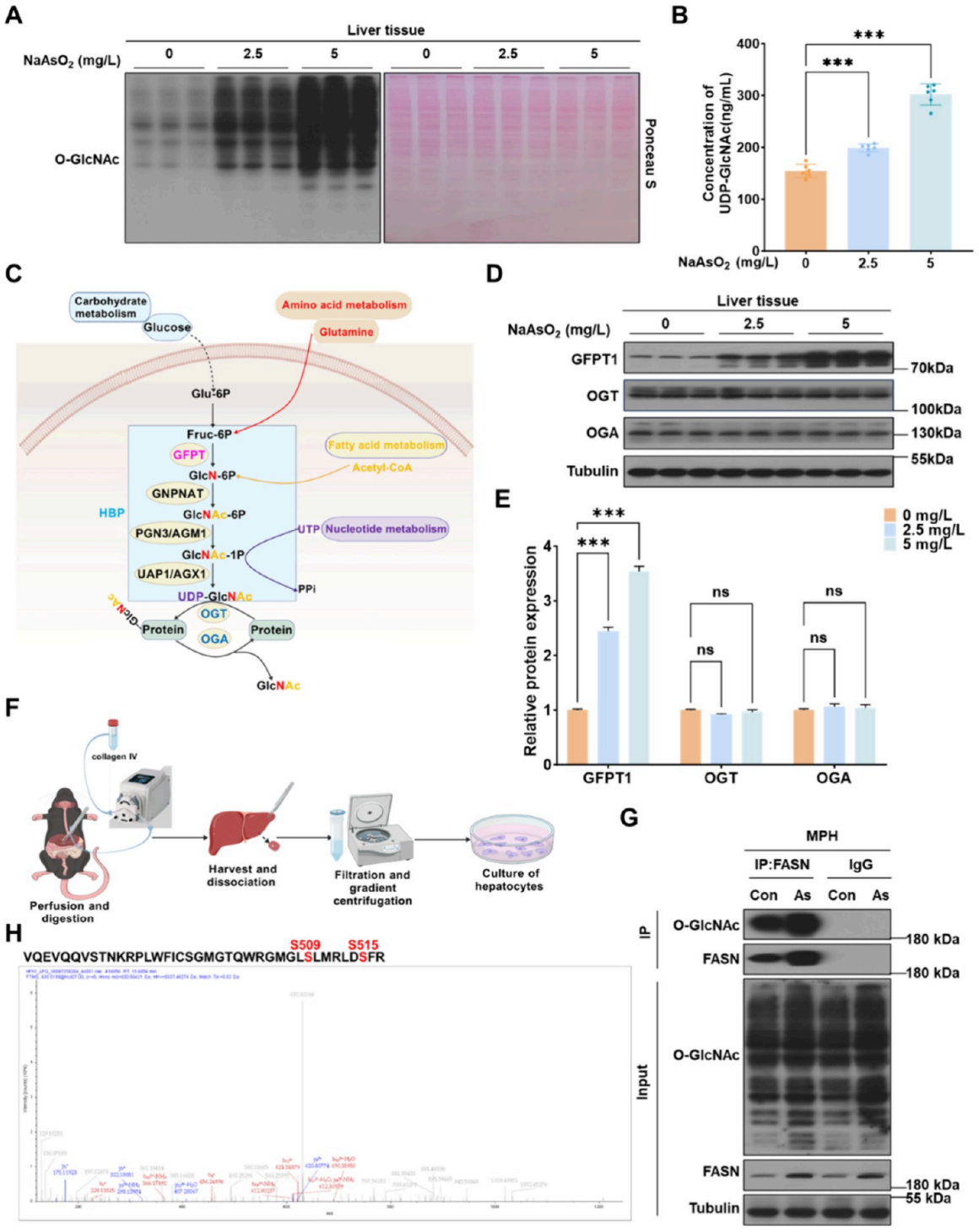

Figure 2. Chronic arsenic exposure activates the HBP pathway and induces O-GlcNAcylation of FASN in livers of mice. C57BL/6J mice were supplied with drinking water containing 0, 2.5, or 5 mg/L $NaAsO_2$ for 6 months. (A) Western blots (left) with corresponding Ponceau S staining (right) for total protein normalization in mouse livers ($n = 6$). (B) Measurement of hepatic UDP-GlcNAc levels in mice ($n = 6$). (C) Schematic diagram depicting the interconnection between the HBP pathway and O-GlcNAcylation. (D) Western blots were prepared, and (E) relative protein levels of GFPT1, OGT, and OGA in the livers were quantified ($n = 6$). Mouse primary hepatocytes were treated with 0 or 2 μM $NaAsO_2$ for 24 h. (F) Schematic diagram of the isolation workflow for mouse primary hepatocytes. (G) Co-IP and Western blot analysis of O-GlcNAcylation levels of FASN in mouse primary hepatocytes ($n = 3$). (H) FASN was purified from mouse primary hepatocytes and analyzed by MS to identify the O-GlcNAcylation sites.

upregulation of FASN protein levels (Figure 1M,N). These findings suggest that arsenic exposure drives hepatic lipid metabolic disorder and lipid accumulation primarily by enhancing fatty acid biosynthesis rather than by suppressing degradation.

3.2. Chronic Arsenic Exposure Activates the HBP Pathway and Induces O-GlcNAcylation of FASN in Livers of Mice

Reported links between O-GlcNAcylation and MASLD prompted us to examine its levels in arsenic-exposed mouse livers.[21,33] Upon arsenic exposure, global O-GlcNAcylation

https://doi.org/10.1021/acs.jafc.6c00603
J. Agric. Food Chem. XXXX, XXX, XXX−XXX

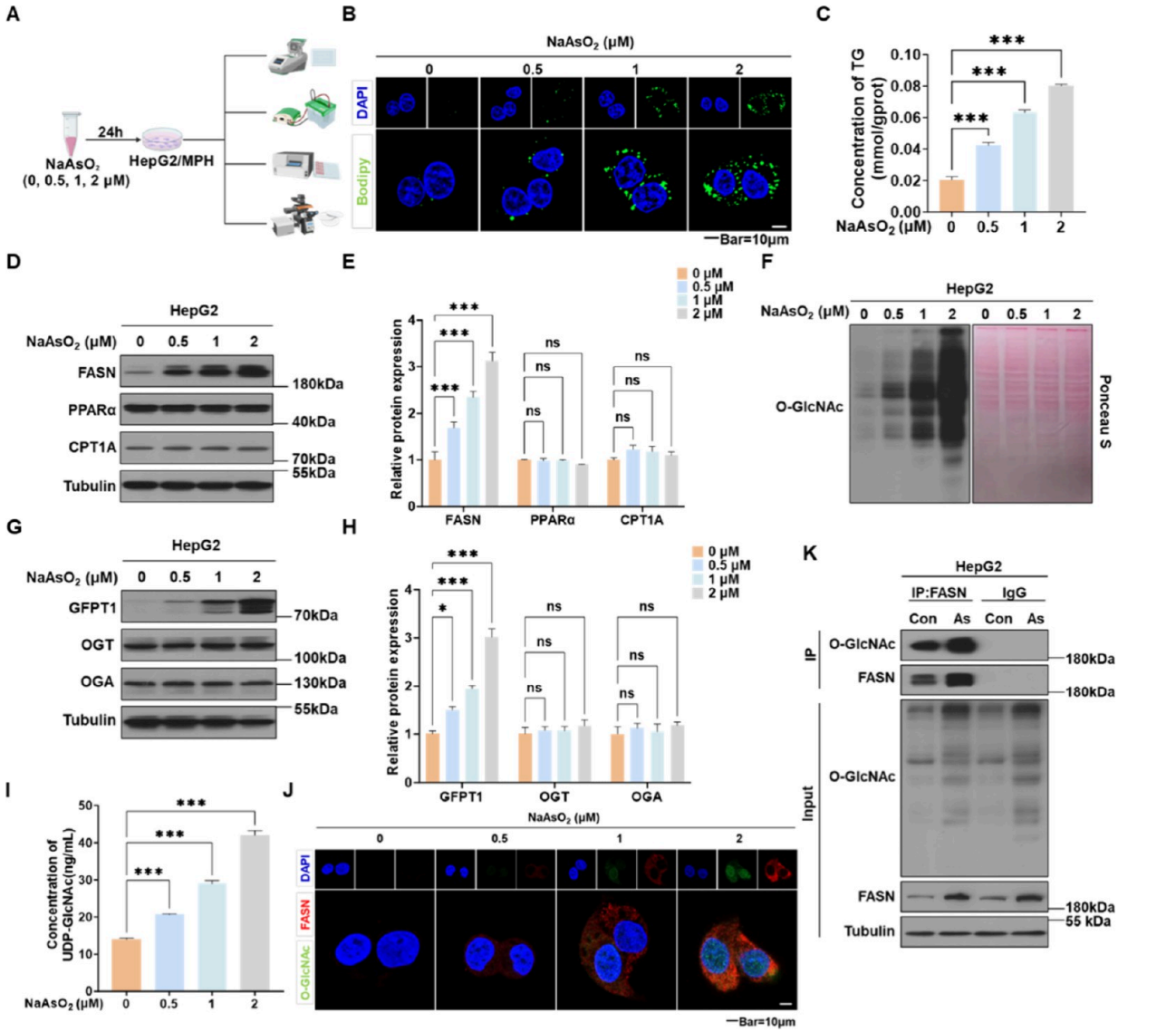

Figure 3. Arsenic induces O-GlcNAcylation of FASN and leads to lipid accumulation in hepatocytes. HepG2 cells were treated with $NaAsO_2$ at concentrations of 0, 0.5, 1, and 2 μM for 24 h. (A) Schematic diagram of arsenic exposure of hepatocytes. (B) Representative confocal images demonstrating BODIPY 493/503-stained lipid droplets in HepG2 cells (n = 3, scale bar = 10 μm). (C) Intracellular TG levels in HepG2 cells (n = 3). (D) Western blots were prepared, and (E) relative protein levels of FASN, PPARα, and CPT1A in HepG2 cells were quantified (n = 3). (F) Western blots (left) with corresponding Ponceau S staining (right) for total protein normalization in HepG2 cells (n = 3). (G) Western blots were prepared, and (H) relative protein levels of GFPT1, OGT, and OGA in HepG2 cells were quantified (n = 3). (I) Measurement of UDP-GlcNAc levels in HepG2 cells (n = 3). (J) IF staining of FASN (red), O-GlcNAc (green), and nuclei with DAPI (blue) in HepG2 cells (n = 3, scale bar = 10 μm). HepG2 cells were treated with $NaAsO_2$ at concentrations of 0 or 2 μM for 24 h. (K) Co-IP and Western blot analysis of O-GlcNAcylation levels of FASN in HepG2 cells (n = 3).

levels were elevated, and the content of the donor substrate UDP-GlcNAc increased in a dose-dependent manner (Figure 2A,B). Although the protein expressions of O-GlcNAc transferase (OGT) and O-GlcNAcase (OGA) remained unchanged, the level of GFPT1 was upregulated (Figure 2C−E). To explore further the regulatory role of O-GlcNAcylation in hepatic lipid accumulation, primary mouse hepatocytes were isolated (Figure 2F). Treatment with 0 or 2 μM $NaAsO_2$ for 24 h followed by Co-IP analysis revealed O-GlcNAcylation on FASN, which was enhanced upon arsenic exposure (Figure 2G). Subsequent MS identified S509 and S515 as functional O-GlcNAcylation sites on FASN (Figure 2H). Our results establish a pathway whereby arsenic exposure upregulates GFPT1 to enhance HBP flux, thereby increasing the supply of UDP-GlcNAc and culminating in elevated O-GlcNAcylation of the FASN protein.

3.3. Arsenic Induces O-GlcNAcylation of FASN and Leads to Lipid Accumulation in Hepatocytes

To establish a cellular model of arsenic exposure, HepG2 cells were treated with 0, 0.5, 1, or 2 μM $NaAsO_2$ for 24 h (Figure 3A). Arsenic exposure induced lipid accumulation, as confirmed by Oil Red O and BODIPY staining (Figure 3B and Figure S2A), and increased intracellular TG levels (Figure 3C). Furthermore, arsenic exposure increased FASN levels without corresponding changes in the expression of fatty acid degradation-related proteins (PPARα and CPT1A) (Figure 3D,E). These results indicate that lipid accumulation in hepatocytes is primarily

https://doi.org/10.1021/acs.jafc.6c00603
J. Agric. Food Chem. XXXX, XXX, XXX−XXX

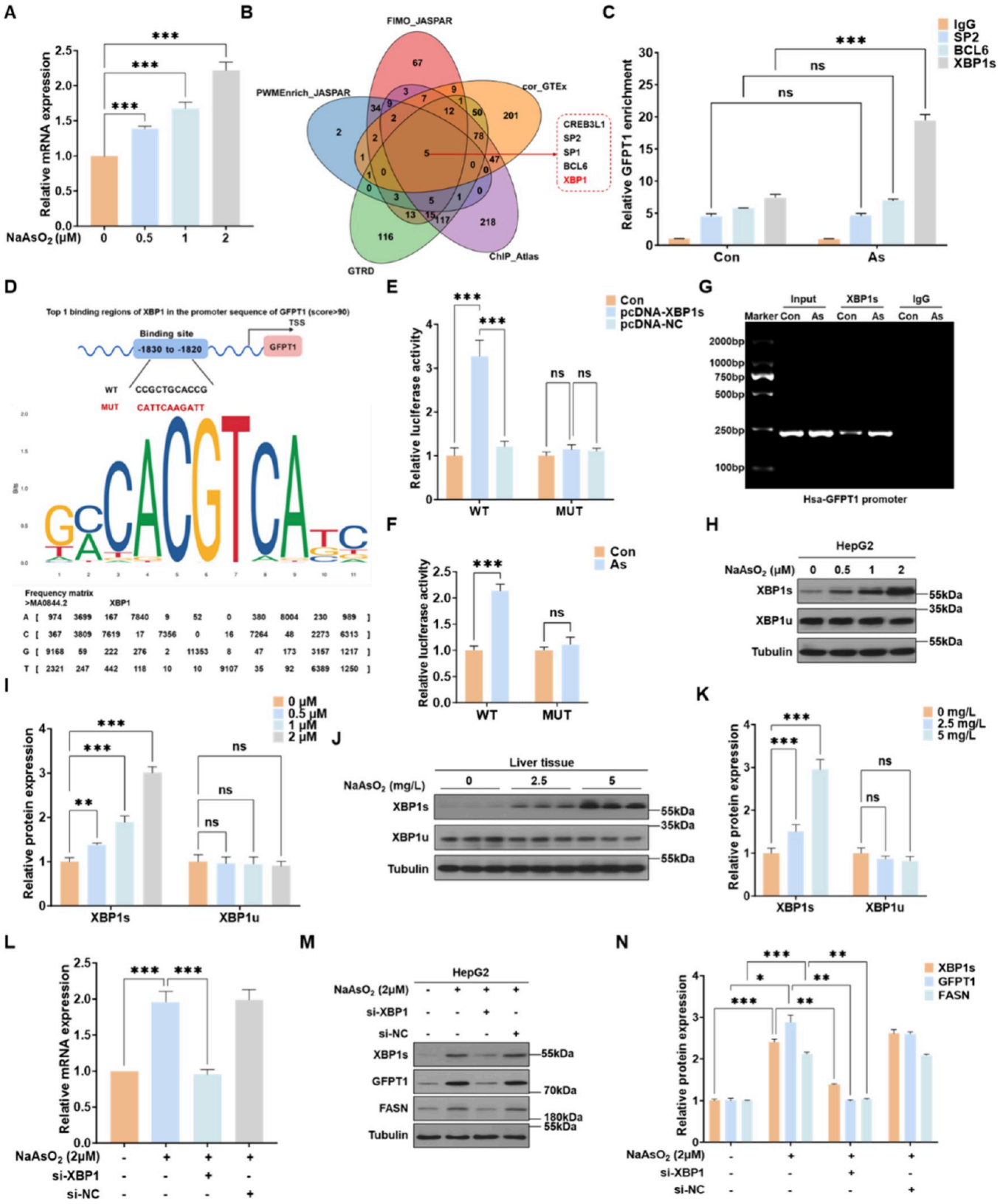

Figure 4. XBP1s induces GFPT1 transcription in arsenic-treated hepatocytes. HepG2 cells were treated with $NaAsO_2$ at concentrations of 0, 0.5, 1, and 2 μM for 24 h. (A) *GFPT1* mRNA levels were measured by qRT-PCR (n = 3). (B) Database predictive analysis identified XBP1 as a potential transcription factor driving GFPT1 expression. Following treatment with 0 or 2 μM $NaAsO_2$, HepG2 cells were harvested for ChIP assays using antibodies against Sp2, BCL6, and XBP1s, with IgG as a negative control. (C) Relative enrichment of *GFPT1* was measured by ChIP-qPCR (n = 3). (D) Wild-type and mutant sequences of the predicted XBP1s binding sites in the GFPT1 promoter region relative to the transcription start site (TSS). (E) Dual-luciferase assay of GFPT1 promoter activity after transfection of reporter plasmids into HepG2 cells (n = 3). HepG2 cells were treated with $NaAsO_2$ at concentrations of 0 or 2 μM for 24 h. (F) Dual-luciferase assay of GFPT1 promoter activity after transfection of reporter plasmids into

https://doi.org/10.1021/acs.jafc.6c00603
J. Agric. Food Chem. XXXX, XXX, XXX−XXX

Figure 4. continued

HepG2 cells ($n = 3$). (G) Endogenous binding of XBP1s to the GFPT1 promoter in HepG2 cells was assessed by ChIP-RT-PCR ($n = 3$). (H) Western blots were prepared, and (I) relative protein levels of XBP1s and XBP1u in HepG2 cells were quantified ($n = 3$). (J) Western blots were prepared, and (K) relative protein levels of XBP1s and XBP1u in the livers were quantified ($n = 6$). HepG2 cells transfected with si-XBP1 or si-NC were treated with 0 or 2 μM $NaAsO_2$ for 24 h. (L) *GFPT1* mRNA levels were measured by qRT-PCR ($n = 3$). (M) Western blots were prepared, and (N) relative protein levels of XBP1s, GFPT1, and FASN in HepG2 cells were quantified ($n = 3$).

promoted by arsenic through the enhancement of fatty acid biosynthesis.

For HepG2 cells, arsenic elevated global O-GlcNAcylation levels (Figure 3F), enhanced GFPT1 protein levels (Figure 3G,H and Figure S2B), and increased its donor substrate, UDP-GlcNAc (Figure 3I). Immunofluorescence (IF) analysis revealed enhanced colocalization of FASN and O-GlcNAc signals with increasing arsenic concentrations (Figure 3J). Co-IP experiments confirmed an interaction between FASN and O-GlcNAcylation, indicating that arsenic promotes the O-GlcNAcylation of FASN (Figure 3K). Consistent with the *in vivo* findings, arsenic exposure activated the HBP pathway through GFPT1 upregulation, which enhanced FASN O-GlcNAcylation to promote fatty acid synthesis and lipid accumulation in the hepatocytes.

3.4. XBP1s Induces GFPT1 Transcription in Arsenic-Treated Hepatocytes

Investigation into the elevated GFPT1 protein levels revealed that arsenic upregulates GFPT1 transcription, as shown by increased mRNA in HepG2 cells (Figure 4A). A multidatabase screening (PWMEnrich-JASPAR, FIMO-JASPAR, cor-GTEx, ChIP-Atlas, GTRD) identified five transcription factors, including CREB3L1, SP2, SP1, BCL6, and XBP1, as potential regulators of GFPT1 upregulation in arsenic-induced MASLD (Figure 4B). Correlation analysis based on the GEPIA database of liver tissue expression revealed that SP2, BCL6, and XBP1 showed relatively high correlations ($R > 0.5$) with GFPT1 expression (Figure S3A-E). Since XBP1 requires splicing into XBP1s to exert its transcriptional activity,[34] we performed ChIP assays using an XBP1s-specific antibody. ChIP-qPCR results demonstrated that arsenic exposure specifically enhanced the enrichment of XBP1s at the GFPT1 promoter region (Figure 4C), suggesting that XBP1s is a transcription factor regulating GFPT1 expression. Using the JASPAR database, we predicted potential XBP1s binding sites in the GFPT1 promoter and selected a site with a score above 90 for validation (Figure 4D). Dual-luciferase reporter assays showed that mutation of this site abolished XBP1s-mediated transcriptional activation of GFPT1 (Figure 4E). Furthermore, arsenic treatment enhanced XBP1s-induced luciferase activity; this effect was absent in the mutant construct (Figure 4F). Subsequent ChIP assays confirmed that treatment of HepG2 cells with 2 μM $NaAsO_2$ for 24 h led to enrichment of the GFPT1 promoter region with the XBP1s antibody (Figure 4G), indicating that arsenic promotes the binding of XBP1s to the GFPT1 promoter.

Additionally, an increase in XBP1s protein levels was evident in both arsenic-treated HepG2 cells and mouse liver tissues (Figure 4H−K). Consistent with this, p-IRE1α was also elevated (Figure S4A−D), indicating involvement of the upstream splicing pathway. Knockdown of XBP1 attenuated the arsenic-induced upregulation of GFPT1 expression (Figure 4L−N and Figure S4E), as well as the increase in global O-GlcNAcylation levels (Figure S4F), UDP-GlcNAc accumulation (Figure S4G), and lipid accumulation in hepatocytes (Figure S4H−J). These findings indicate that XBP1s directly binds to the GFPT1 promoter to stimulate its transcription, thereby contributing to GFPT1 overexpression in arsenic-induced MASLD.

3.5. O-GlcNAcylation of FASN S509 Is Involved in Arsenic-Induced Lipid Accumulation in Hepatocytes through Inhibiting Its Ubiquitination and Thereby Enhancing Protein Stability

To elucidate the mechanism by which O-GlcNAcylation upregulates FASN protein levels, we performed protein stability assays. HepG2 cells were treated with 0 or 2 μM $NaAsO_2$ in the presence of cycloheximide (CHX) to inhibit protein synthesis, and FASN protein levels were measured at selected time points. Arsenic exposure prolonged the half-life of FASN protein (Figure 5A,B). We treated both normal and arsenic-exposed HepG2 cells with benzyl-α-GalNAc (BAGN), an O-GlcNAcylation inhibitor. BAGN suppressed the arsenic-induced increase in both global O-GlcNAcylation levels (Figure S5A). Furthermore, BAGN blocked the upregulation of FASN protein and the consequent lipid accumulation (including elevated levels of TG) induced by arsenic exposure (Figure S5B−F). To identify the degradation pathway through which O-GlcNAcylation regulates FASN, we treated HepG2 cells with 0 or 2 μM $NaAsO_2$ in combination with the ubiquitin−proteasome inhibitor MG132, the autophagy−lysosome inhibitor chloroquine (CQ), or the O-GlcNAcylation inhibitor BAGN. Only MG132 reversed the BAGN-induced decrease in FASN protein levels (Figure 5C,D), showing that arsenic stabilizes FASN by suppressing its ubiquitin−proteasome-mediated degradation via O-GlcNAcylation. Ubiquitination immunoprecipitation assays confirmed that arsenic exposure reduced FASN ubiquitination (Figure 5E).

Evolutionary conservation analysis of the O-GlcNAcylation sites on FASN identified by MS revealed that the S509 site was highly conserved across species (Figure 5F). We therefore constructed a point mutant plasmid in which serine 509 was replaced by alanine (FASN-S509A), which cannot be O-GlcNAcylated (Figure 5G). Endogenous FASN was knocked down in HepG2 cells (Figure S5G), followed by transfection with the wild-type (FASN-WT) or mutant (FASN-S509A) plasmid and treatment with 0 or 2 μM $NaAsO_2$. The S509 mutation suppressed arsenic-induced O-GlcNAcylation of FASN, increased its ubiquitination, and reversed FASN protein accumulation (Figure 5H,I). Subsequent protein stability assays showed that the FASN-S509A mutation abolished the arsenic-induced extension of FASN protein half-life (Figure 5J,K). Furthermore, this mutation alleviated arsenic-induced elevation of TG levels and lipid accumulation in hepatocytes (Figure 5L and Figure S5H,I). These results demonstrate that arsenic promotes O-GlcNAcylation at S509 of FASN, which inhibits its ubiquitination and degradation, thereby enhancing FASN stability and contributing to lipid accumulation in hepatocytes.

https://doi.org/10.1021/acs.jafc.6c00603
J. Agric. Food Chem. XXXX, XXX, XXX−XXX

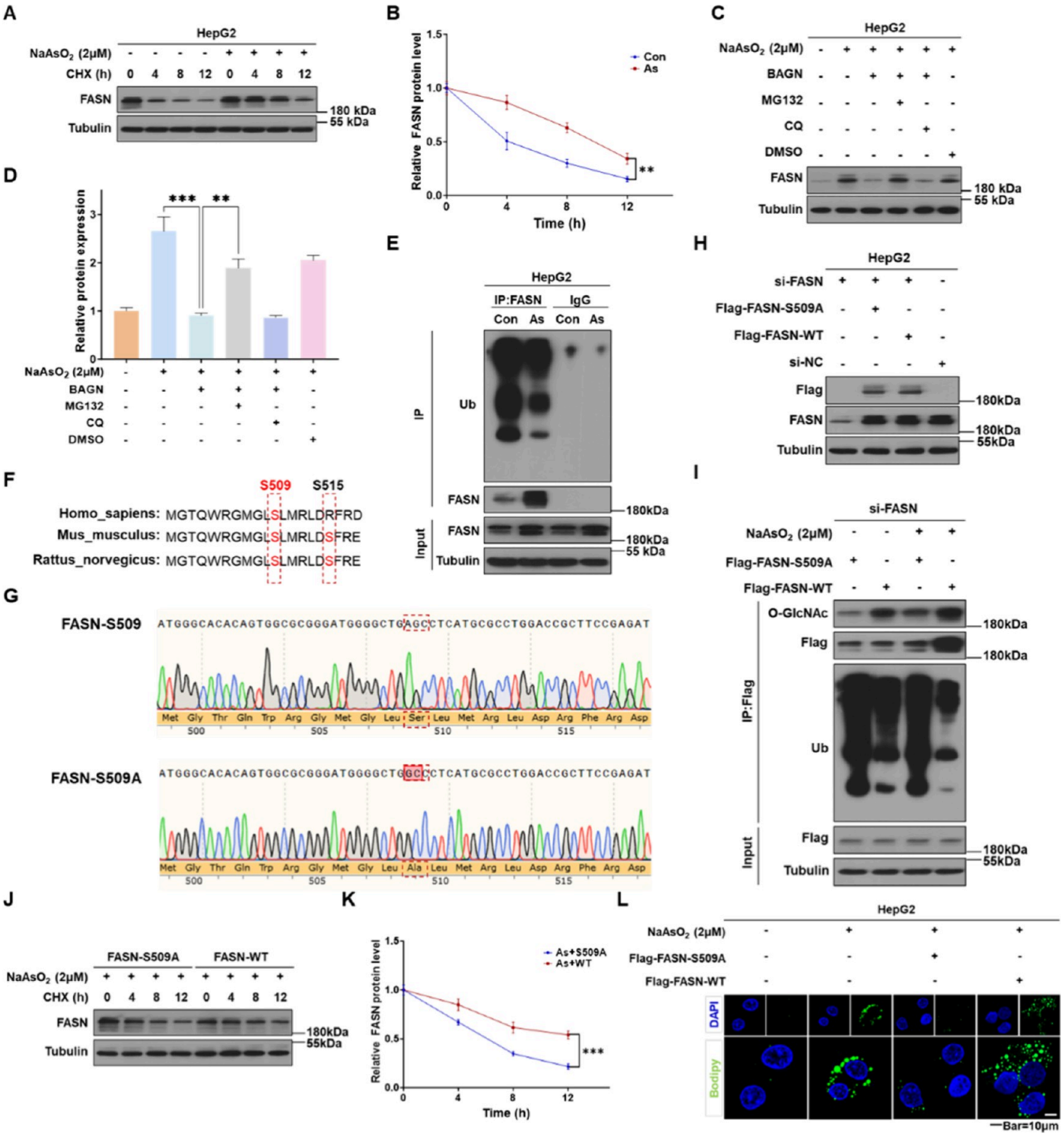

Figure 5. Arsenic exposure-induced O-GlcNAcylation of FASN S509 enhances the protein stability by inhibiting its ubiquitination. HepG2 cells treated with 0 or 2 μM $NaAsO_2$ for 24 h were incubated with CHX and harvested at 0, 4, 8, and 12 h intervals. (A) FASN protein stability was assessed by Western blots. (B) The half-life of FASN in HepG2 cells with the indicated treatments was measured by Western blots. FASN levels were normalized by tubulin, and the 0 h points were set to 100% (n = 3). (C) Western blots were prepared, and (D) relative protein levels of FASN in HepG2 cells were quantified (n = 3). (E) Analysis of FASN ubiquitination by Co-IP and Western blots (n = 3). (F) Comparison of sequence homology at O-GlcNAcylation sites of FASN across various species. (G) Sanger sequencing chromatogram of the site-directed mutant plasmid. Site-directed mutagenesis of FASN at serine 509 to alanine. HepG2 cells were co-transfected with either si-FASN or si-NC and either Flag-FASN-S509A or Flag-FASN-WT. (H) Protein expression was analyzed by Western blots (n = 3). (I) Analysis of Flag-FASN O-GlcNAcylation and ubiquitination in HepG2 cells by Co-IP and Western blots (n = 3). HepG2 cells transfected with Flag-FASN-S509A or Flag-FASN-WT were treated with 2 μM $NaAsO_2$ for 24 h, and FASN protein stability was assessed by Western blots. (J) Protein synthesis was blocked by CHX for the indicated times. (K) Half-life of FASN in HepG2 cells with the indicated treatments as measured by Western blots. FASN levels were normalized by tubulin, and the 0 h points were set to 100% (n = 3). (L) Representative confocal images demonstrating BODIPY 493/503-stained lipid droplets in HepG2 cells (n = 3, scale bar = 10 μm).

https://doi.org/10.1021/acs.jafc.6c00603
J. Agric. Food Chem. XXXX, XXX, XXX−XXX

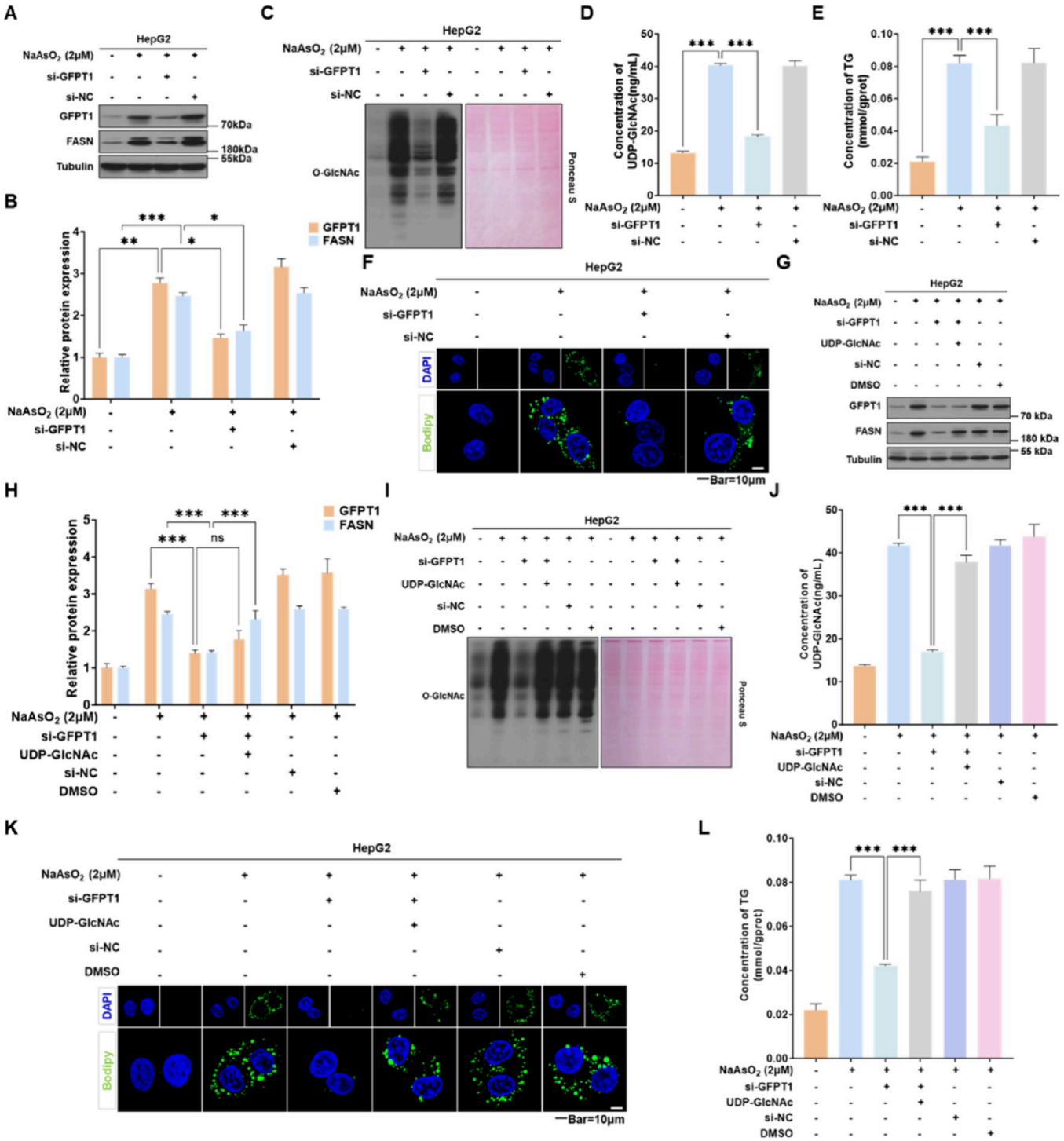

Figure 6. GFPT1 contributes to arsenic-induced O-GlcNAcylation of FASN and lipid accumulation by mediating UDP-GlcNAc production in hepatocytes. HepG2 cells transfected with si-GFPT1 or si-NC were treated with 0 or 2 μM $NaAsO_2$ for 24 h. (A) Western blots were prepared, and (B) relative protein levels of GFPT1 and FASN in HepG2 cells were quantified (n = 3). (C,I) Western blots (left) with corresponding Ponceau S staining (right) for total protein normalization in HepG2 cells (n = 3). (D,J) Measurement of UDP-GlcNAc levels in HepG2 cells (n = 3). (E,L) Intracellular TG levels in HepG2 cells (n = 3). (F,K) Representative confocal images demonstrating BODIPY 493/503-stained lipid droplets in HepG2 cells (n = 3, scale bar = 10 μm). HepG2 cells were transfected with si-GFPT1 and treated with or without UDP-GlcNAc and then exposed to 2 μM $NaAsO_2$ for 24 h. (G) Western blots were prepared, and (H) relative protein levels of GFPT1 and FASN in HepG2 cells were quantified (n = 3).

3.6. GFPT1 Contributes to Arsenic-Induced O-GlcNAcylation of FASN and Lipid Accumulation by Mediating UDP-GlcNAc Production in Hepatocytes

To examine the involvement of the GFPT1-driven HBP pathway in hepatic lipid dysregulation caused by arsenic, we generated a GFPT1-knockdown model with HepG2 cells using siRNA (si-GFPT1) and verified its knockdown efficiency (Figure 6A,B and Figure S6A). Cells were transfected with the most effective si-GFPT1 or control si-NC, followed by treatment with 0 or 2 μM $NaAsO_2$ for 24 h. GFPT1 knockdown

https://doi.org/10.1021/acs.jafc.6c00603
J. Agric. Food Chem. XXXX, XXX, XXX−XXX

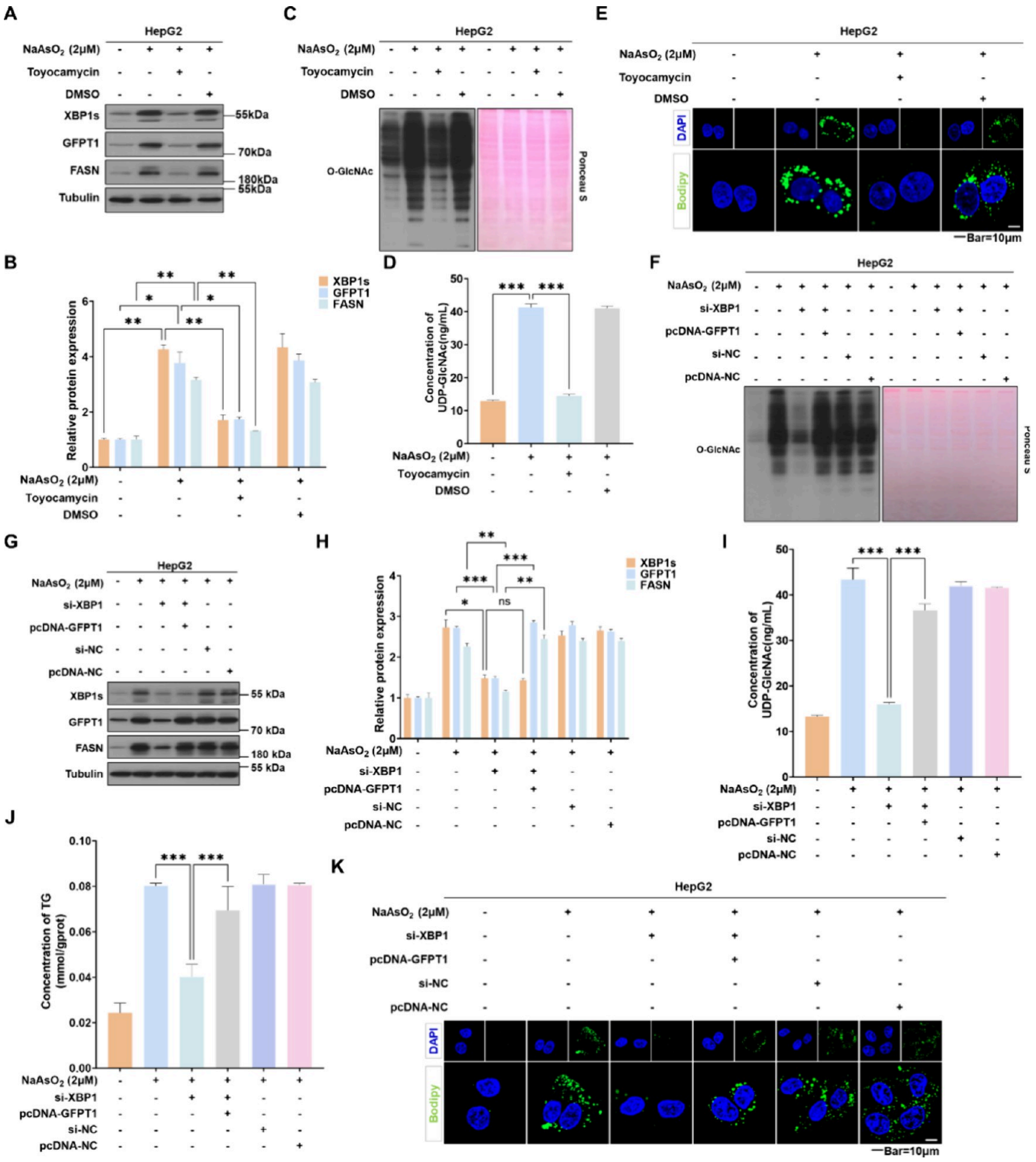

Figure 7. XBP1s is involved in arsenic-induced lipid accumulation through regulating GFPT1 expression and facilitating FASN O-GlcNAcylation in hepatocytes. HepG2 cells were treated with or without toyocamycin and then exposed to 0 or 2 μM $NaAsO_2$ for 24 h. (A) Western blots were prepared, and (B) relative protein levels of XBP1s, GFPT1, and FASN in HepG2 cells were quantified (n = 3). (C,F) Western blots (left) with corresponding Ponceau S staining (right) for total protein normalization in HepG2 cells (n = 3). (D,I) Measurement of UDP-GlcNAc levels in HepG2 cells (n = 3). (E,K) Representative confocal images demonstrating BODIPY 493/503-stained lipid droplets in HepG2 cells (n = 3, scale bar = 10 μm). HepG2 cells were transfected either with si-XBP1 or co-transfected with si-XBP1 and pcDNA-GFPT1 for 24 h, followed by arsenic exposure (2 μM) for 24 h. (G) Western blots were prepared, and (H) relative protein levels of XBP1s, GFPT1, and FASN in HepG2 cells were quantified (n = 3). (J) Intracellular TG levels in HepG2 cells (n = 3).

abolished the upregulation of global O-GlcNAcylation and UDP-GlcNAc synthesis induced by arsenic (Figure 6C,D). Downregulation of GFPT1 also blocked arsenic-induced lipid accumulation in HepG2 cells, as well as the increases in

https://doi.org/10.1021/acs.jafc.6c00603
J. Agric. Food Chem. XXXX, XXX, XXX−XXX

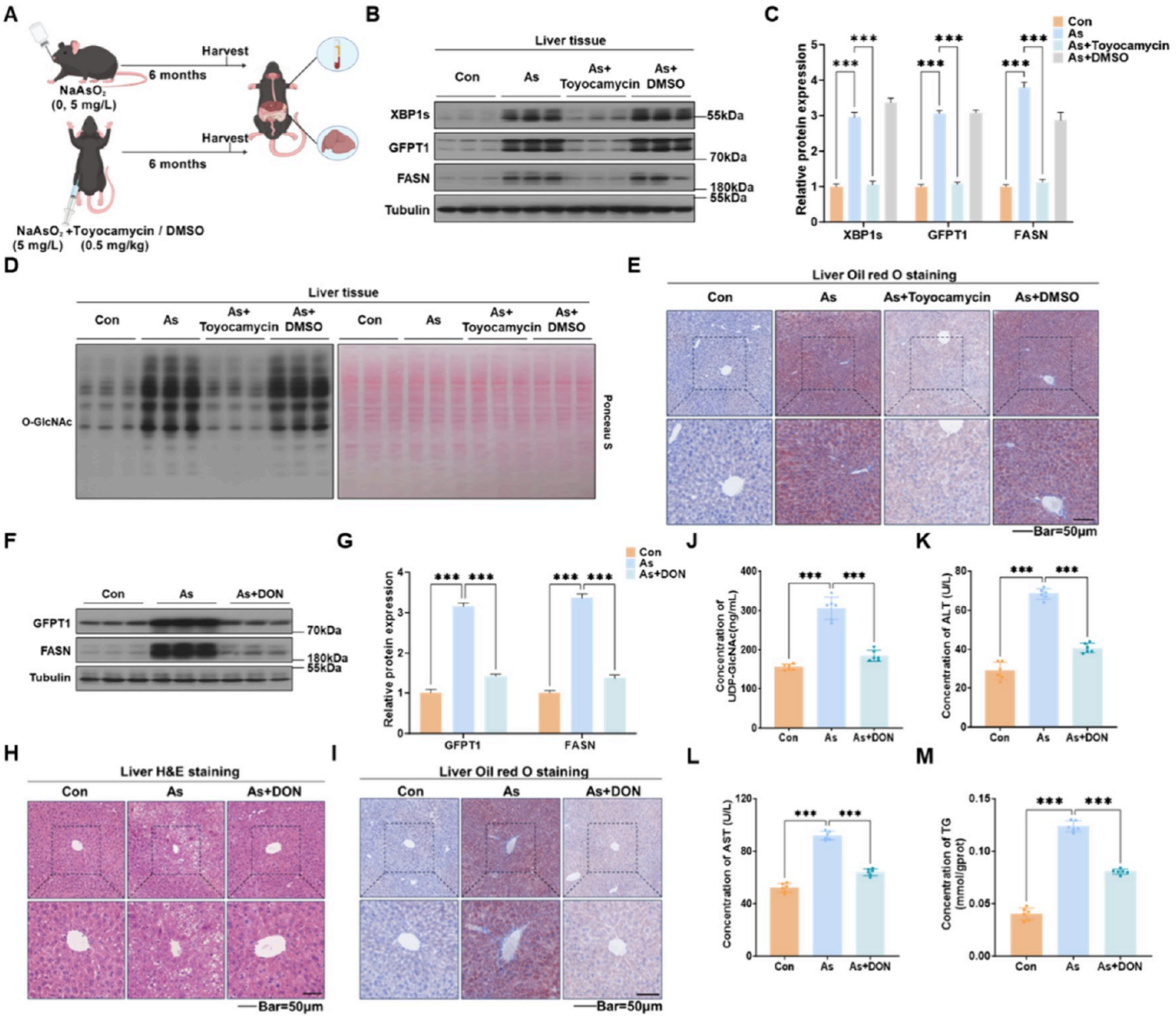

Figure 8. Intervention with either toyocamycin or DON alleviates chronic arsenic exposure-induced MASLD in mice. C57BL/6J mice received 0 or 5 mg/L $NaAsO_2$ in their drinking water for 6 months, along with weekly intraperitoneal injections of toyocamycin (0.5 mg/kg) or DMSO. (A) Schematic of the experimental model for toyocamycin intervention in mice. (B) Western blots were prepared, and (C) relative protein levels of XBP1s, GFPT1, and FASN in the liver were quantified (n = 6). (D) Western blots (left) with corresponding Ponceau S staining (right) for total protein normalization in mouse livers (n = 6). (E) Representative Oil Red O-stained liver sections (n = 6, scale bar = 50 μm). C57BL/6J mice received 0 or 5 mg/L $NaAsO_2$ in their drinking water for 6 months, along with weekly intraperitoneal injections of DON (1 mg/kg). (F) Western blots were prepared, and (G) relative protein levels of GFPT1 and FASN in the liver were quantified (n = 6). (H) Representative H&E-stained liver sections (n = 6, scale bar = 50 μm). (I) Representative Oil Red O-stained liver sections (n = 6, scale bar = 50 μm). (J) Measurement of hepatic UDP-GlcNAc levels in mice (n = 6). The serum levels of ALT (K) and AST (L) and the hepatic levels of TG (M) in mice were measured (n = 6).

downstream FASN protein expression and TG levels (Figure 6E,F and Figure S6B). Compared to the arsenic-only group, cells co-treated with the HBP-specific inhibitor DON exhibited reduced O-GlcNAcylation levels and lower UDP-GlcNAc contents (Figure S6C,D). We also treated normal and arsenic-exposed HepG2 cells with DON, which inhibited the arsenic-induced upregulation of GFPT1 and FASN protein levels (Figure S6E,F). Moreover, DON counteracted the lipid deposition and elevated the lipid profile triggered by arsenic exposure (Figure S6G−I). These results indicate that inhibition of GFPT1 activity suppresses UDP-GlcNAc production, thereby blocking arsenic-induced O-GlcNAcylation of FASN and subsequent lipid accumulation.

Then, we conducted a rescue experiment to validate the role of GFPT1-regulated HBP flux in arsenic-induced hepatic lipid accumulation. After transfecting HepG2 cells with si-GFPT1, exogenous UDP-GlcNAc was added during arsenic exposure. The suppression of O-GlcNAcylation and FASN protein levels induced by GFPT1 knockdown was reversed by exogenous UDP-GlcNAc supplementation (Figure 6G−J). Consistently, the attenuation of lipid accumulation resulting from GFPT1 knockdown was also restored upon UDP-GlcNAc treatment (Figure 6K,L and Figure S6J). Collectively, these findings demonstrate that GFPT1 promotes UDP-GlcNAc production via the HBP pathway, thereby contributing to increased O-

https://doi.org/10.1021/acs.jafc.6c00603
J. Agric. Food Chem. XXXX, XXX, XXX−XXX

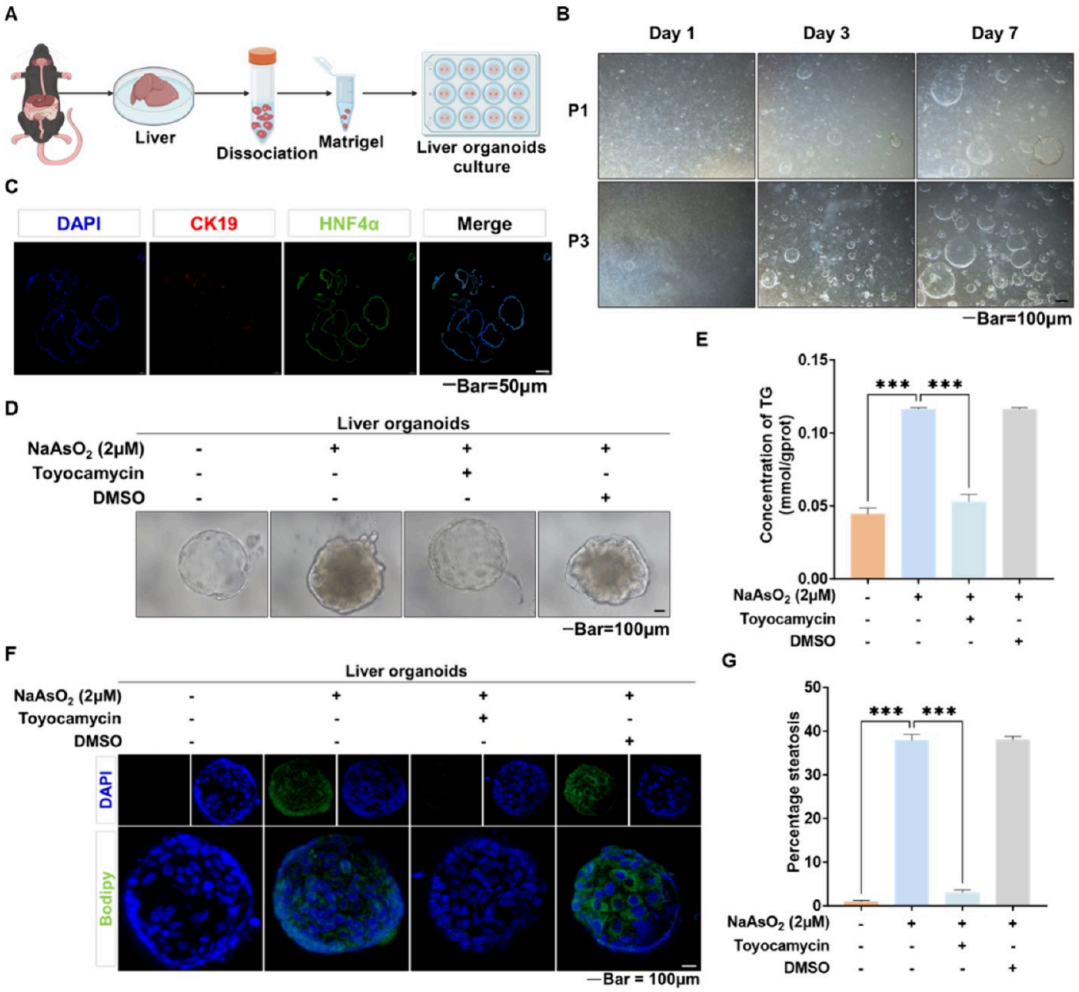

Figure 9. The inhibition of XBP 1s effectively alleviates arsenic-induced steatosis in liver organoids. (A) Schematic diagram of the construction process of mouse liver organoids. (B) Representative bright-field images of liver organoids (n = 3, scale bar = 100 μm). (C) IF staining of CK19 (red), HNF4α (green), and nuclei with DAPI (blue) in liver organoids (n = 3, scale bar = 50 μm). Liver organoids were treated with or without toyocamycin and then exposed to 0 or 2 μM $NaAsO_2$ for 24 h. (D) Representative bright-field images of liver organoids (n = 3, scale bar = 100 μm). (E) The levels of TG in liver organoids (n = 3). (F) Representative confocal images demonstrating BODIPY 493/503-stained lipid droplets in liver organoids (n = 3, scale bar = 100 μm). (G) Quantification of the percentage of steatosis in liver organoids (n = 3).

GlcNAcylation of FASN and lipid accumulation in hepatocytes induced by arsenic exposure.

3.7. XBP1s Is Involved in Arsenic-Induced Lipid Accumulation through Regulation of GFPT1 Expression and Facilitation of FASN O-GlcNAcylation in Hepatocytes

To assess the contribution of XBP1s in arsenic-induced lipid deposition in hepatocytes, control or arsenic-exposed HepG2 cells were treated with toyocamycin to inhibit XBP1 splicing. This treatment prevented the upregulation of GFPT1 and FASN protein levels induced by arsenic (Figure 7A,B). Compared to the arsenic-only treatment group, cells co-treated with toyocamycin exhibited reduced O-GlcNAcylation levels and lower content of its donor substrate, UDP-GlcNAc (Figure 7C,D). Furthermore, toyocamycin blocked the arsenic-induced lipid accumulation in HepG2 cells, as well as the elevations of intracellular TG levels (Figure 7E and Figure S7A,B).

To characterize the mechanism by which XBP1s regulates GFPT1 in arsenic-induced lipid accumulation, we performed a rescue experiment by transfecting HepG2 cells with si-XBP1 alone or together with a GFPT1 overexpression plasmid (pcDNA-GFPT1), followed by treatment with 0 or 2 μM $NaAsO_2$ for 24 h. This approach allowed us to examine the effects of restoring GFPT1 expression after transcriptional suppression. The results showed that the pcDNA-GFPT1 plasmid increased GFPT1 protein levels in cells (Figure S7C,D). The suppression of GFPT1 expression and O-GlcNAcylation induced by XBP1 knockdown was reversed by GFPT1 re-expression (Figure 7F−I); the attenuation of lipid accumulation was also restored (Figure 7J,K and Figure S7E). These findings indicate that XBP1s contributes to arsenic-induced lipid deposition in hepatocytes by regulating GFPT1 expression, thereby influencing downstream O-GlcNAcylation of FASN.

3.8. Intervention with Either Toyocamycin or DON Alleviates Chronic Arsenic Exposure-Induced MASLD in Mice

To validate these findings *in vivo*, we established an arsenic-exposed mouse model with toyocamycin intervention via intraperitoneal injection (Figure 8A). Toyocamycin treatment prevented the upregulation of hepatic XBP1s, GFPT1, and FASN protein levels induced by arsenic (Figure 8B,C), as well as the elevation of O-GlcNAcylation (Figure 8D), without altering the liver-to-body weight ratio (Figure S8A). Consistent with this, toyocamycin reversed the arsenic-induced elevation of UDP-GlcNAc content in liver tissue (Figure S8B). Toyocamy-

https://doi.org/10.1021/acs.jafc.6c00603
J. Agric. Food Chem. XXXX, XXX, XXX−XXX

cin also reduced serum ALT and AST levels in arsenic-exposed mice (Figure S8C,D). Histopathological examination showed that, for hepatocytes, toyocamycin intervention alleviated arsenic-induced vacuolar degeneration (Figure S8E,F). Oil Red O staining confirmed that toyocamycin attenuated arsenic-induced hepatic steatosis (Figure 8E and Figure S8G). Hepatic TG levels were lower in the toyocamycin intervention group compared to those in the arsenic-only group (Figure S8H). These results show that toyocamycin ameliorates chronic arsenic-induced hepatic lipid accumulation in mice by inhibiting the XBP1 splicing.

To confirm the role of the HBP pathway in animals, we established a mouse model of arsenic exposure with DON intervention via intraperitoneal injection (Figure S9A). The liver-to-body weight ratios were unaffected by DON intervention (Figure S9B). However, DON suppressed the elevated hepatic GFPT1 protein and O-GlcNAcylation levels and blocked FASN upregulation, induced by arsenic (Figure 8F,G and Figure S9C). Similarly, for arsenic-exposed mice, DON alleviated hepatocellular vacuolation (Figure 8H and Figure S9D) and suppressed hepatic lipid accumulation (Figure 8I and Figure S9E). It also inhibited the arsenic-induced elevation of hepatic UDP-GlcNAc levels (Figure 8J) and the reduced serum ALT and AST levels (Figure 8K,L). Furthermore, hepatic TG levels were lower in the DON intervention group compared with the arsenic-only group (Figure 8M). These results demonstrate that DON blocks chronic arsenic-induced hepatic lipid accumulation by inhibiting the HBP pathway.

3.9. The Inhibition of XBP1s Effectively Alleviates Arsenic-Induced Steatosis in Liver Organoids

Following previously established methodology,[35] we generated and characterized mouse liver organoids (Figure 9A). The organoids grew well in bright-field view and expressed both the cholangiocyte marker CK19 and the mature hepatocyte marker HNF4α, further confirming the successful model establishment (Figure 9B,C). We then treated the organoids, with or without arsenic exposure, using the XBP1s inhibitor toyocamycin. Arsenic led to visible darkening of the hepatic organoids and elevated the levels of TG, with BODIPY staining further confirming increased lipid accumulation. Compared to the arsenic-only group, toyocamycin co-treatment markedly reduced TG content and the extent of steatosis, and partially restored their morphology (Figure 9D−G). These results confirm that inhibition of XBP1s alleviates arsenic-induced lipid accumulation in liver organoids, in line with our prior evidence from animal and cellular models.

4. DISCUSSION

In 2023, three major international liver associations put forward the proposal of substituting MASLD for nonalcoholic fatty liver disease (NAFLD). Epidemiological evidence demonstrates excellent congruence between NAFLD and MASLD definitions, with more than 99% of individuals diagnosed with NAFLD meet the diagnostic standards for MASLD.[36,37] The onset and progression of MASLD are driven by a complex interplay of genetic, metabolic, lifestyle, and environmental factors.[36] In recent years, exposure to environmental pollutants has drawn increasing concern as an exogenous risk factor for MASLD. Endocrine-disrupting chemicals (EDCs), such as bisphenol A and phthalates, contribute to hepatic steatosis and inflammation through mechanisms involving oxidative stress and mitochondrial dysfunction.[38,39] Our findings demonstrate that arsenic disrupts hepatic lipid metabolism and induces lipid accumulation in hepatocytes, observations that align with previous studies establishing arsenic as an independent risk factor for NAFLD.[8] Although evidence linking arsenic exposure to MASLD is still emerging, our findings and other epidemiological work point to environmental factors, with arsenic as a contributor.

FASN is a multifunctional cytosolic enzyme that drives the rate-limiting step in *de novo* lipogenesis.[40] It primarily utilizes NADPH as a reducing equivalent to convert malonyl-CoA and acetyl-CoA to palmitate.[41] Our proteomic analyses revealed the upregulation of hepatic FASN in a chronic arsenic-exposure mouse model, suggesting its importance in the pathogenesis of arsenic-induced MASLD. FASN is regulated not only transcriptionally by SREBP-1c but also post-translationally via modifications that alter its stability and activity.[42] O-GlcNAcylation is involved in maintaining metabolic homeostasis, and its dysregulation is associated with MASLD development.[21,43] Notably, arsenic elevates global O-GlcNAcylation and impairs insulin signaling via the AMPK/mTOR-autophagy pathway.[44] Consistent with this, we found, through co-immunoprecipitation and co-localization assays, that arsenic elevated O-GlcNAcylation in hepatocytes and confirmed that FASN is an O-GlcNAcylated target. MS identified Ser509 as a functional O-GlcNAcylated site on FASN, and its mutation abolished arsenic-induced lipid deposition. These results establish the essential action of O-GlcNAcylation in regulating FASN function and provide experimental evidence for understanding how environmental arsenic exposure disrupts lipid metabolism on the molecular level.

Metabolic reprogramming allows cells to adapt their metabolic networks in response to environmental stress. Arsenic exposure disrupts energy homeostasis and alters lipid and amino acid metabolism.[6,12] The conversion of 2−5% of glucose to UDP-GlcNAc via the HBP pathway is accomplished by the rate-limiting enzyme GFPT1. Catalyzed by OGT and OGA, O-GlcNAcylation is a modification that requires UDP-GlcNAc as a donor.[16,45] Elevated O-GlcNAcylation has been linked to diabetic retinopathy, and endothelial-specific OGT knockout or inhibition ameliorates vascular dysfunction.[46] We propose that arsenic enhances O-GlcNAcylation by increasing substrate supply via the HBP pathway, despite unaltered OGT/OGA expression. This is likely accomplished by GFPT1, which controls the flux-controlling step for UDP-GlcNAc synthesis in the HBP, thereby driving substrate availability.

GFPT1 serves as the primary rate-limiting enzyme in the HBP pathway, converting glutamine and fructose-6-phosphate into glucosamine-6-phosphate. GFPT1 upregulation-mediated HBP pathway activation and subsequent O-GlcNAcylation of the transcription factor VEZF1 are instrumental in the malignant progression of hepatocellular carcinoma.[47] We demonstrated that arsenic increased hepatic UDP-GlcNAc and GFPT1 expression, showing that the GFPT1-driven HBP flux underlies arsenic-induced metabolic reprogramming. DON blocked arsenic-induced GFPT1 expression and the ensuing O-GlcNAcylation-dependent lipogenesis. Similarly, in mesenchymal stem cells, a reduced HBP flux decreases UDP-GlcNAc synthesis and modulates O-GlcNAcylation of FOXO3 S296 to inhibit osteogenic differentiation.[48] These findings establish that UDP-GlcNAc, produced via the GFPT1-mediated HBP pathway, acts as a biomarker of arsenic-induced metabolic disruption and as a contributor to MASLD pathogenesis.

https://doi.org/10.1021/acs.jafc.6c00603
J. Agric. Food Chem. XXXX, XXX, XXX−XXX

Beyond nutrient levels, O-GlcNAcylation is responsive to diverse cellular stresses, including hypoxia, heat shock, and nutrient deprivation, although the underlying mechanisms remain incompletely understood.[49] The unfolded protein response is a cellular pathway activated by accumulation of misfolded proteins during stress, which maintains proteostasis. The IRE1α branch, central to this process, orchestrates the unconventional splicing of *XBP1u* (transcriptionally inert) mRNA to produce transcriptionally active *XBP1s*.[50] In the present study, screening of the GFPT1 upstream promoter identified potential XBP1s binding motifs. Combined dual-luciferase reporter and ChIP assays established GFPT1 as a direct transcriptional target of XBP1s, corroborating previous findings.[51] Furthermore, activation of the IRE1α/XBP1s axis by arsenite in the vascular endothelium aligns with our observation of its activation in arsenic-exposed liver tissues and hepatocytes.[52] We established that XBP1 inhibition or knockdown attenuates GFPT1-mediated UDP-GlcNAc synthesis and O-GlcNAcylation, thus preventing arsenic-induced lipid accumulation. Rescue experiments confirmed that GFPT1 acts downstream of XBP1, as its overexpression compensated for the loss of XBP1 in maintaining HBP flux and lipid homeostasis. These results confirm that GFPT1 upregulation is not an isolated event but a component of the adaptive metabolic reprogramming mediated by XBP1s under arsenic exposure.

O-GlcNAcylation is a crucial nutrient-sensitive post-translational modification that regulates protein stability through both the ubiquitin-proteasome pathway and the autophagy-lysosome pathway.[53] Within the ubiquitin-proteasome system, O-GlcNAcylation stabilizes the transferrin receptor via inhibited ubiquitination to promote iron accumulation and ferroptosis in hepatocellular carcinoma, suggesting a new treatment strategy.[54] Site-specific O-GlcNAcylation promotes NAFLD progression by stabilizing CD36 and blocking its ubiquitin-dependent degradation.[55] O-GlcNAcylation of ENO1 S249 stabilizes programmed death-ligand 1 (PD-L1) by blocking its STUB1-mediated ubiquitination and degradation, thereby upregulating its expression and promoting PD-1/PD-L1-dependent immune escape.[56] Through the autophagy-lysosome pathway, O-GlcNAcylation stabilizes GATA4 by blocking its p62-mediated autophagic degradation, thereby promoting GATA4 accumulation to drive the senescence-associated secretory phenotype and to exacerbate osteoarthritis.[57] Similarly, for multiple myeloma, O-GlcNAcylation stabilizes CDC27, and the OGT inhibitor OSMI-1 induces its degradation through the autophagy-lysosome pathway.[58] Our results demonstrate that arsenic stabilizes FASN through S509 O-GlcNAcylation to block ubiquitin-proteasome degradation, with the S509 mutation confirming this mechanism by enhancing the level of ubiquitination and reducing protein stability. These results elucidate the involvement of O-GlcNAcylation in regulating FASN protein stability via the ubiquitin-proteasome pathway in arsenic-induced hepatic lipid accumulation.

Liver organoids demonstrate significant advantages as alternatives to traditional animal and human experiments. Notably, 3D culture models are particularly promising because of their superior physiological relevance and translational potential. These models more accurately recapitulate liver tissue heterogeneity, organotypic architecture, and metabolic functions.[59] They substantially reduce the reliance on live animal studies while providing a reproducible and controllable *in vitro* platform for human-specific research. Such advancements have enabled robust disease modeling and drug screening in adult liver organoids.[60] Recent research utilizing a 3D murine liver organoid platform has demonstrated its utility in studying lipid metabolism and assessing metabolites of EDCs.[61] In this study, we established a liver organoid model and found that inhibition of XBP1s significantly alleviated arsenic-induced steatosis, suggesting XBP 1s as a potential therapeutic target for arsenic-associated MASLD. This highlights the value of organoid models in replacing complex *in vivo* experiments for mechanistic investigations and target identification.

In addition to the XBP1s-GFPT1-FASN axis identified here, hepatic lipid metabolism involves complex signaling networks. Classically, SREBP-1c drives transcription of lipogenic genes, including FASN in response to insulin and nutrient excess.[62] Our previous work demonstrated that arsenic activates SREBP-1c, which may contribute to increased *FASN* mRNA.[30] As a key energy sensor, AMPK negatively regulates fatty acid synthesis via phosphorylation of acetyl-CoA carboxylase (ACC) or inhibition of SREBP-1c activity,[63,64] and arsenic may suppress AMPK signaling as reported for other models.[65] At the catabolic level, PPARα promotes fatty acid oxidation and counteracts lipid accumulation.[66] Although, in our study, arsenic did not alter PPARα protein levels, whether it affects PPARα transcriptional activity requires further investigation. However, how arsenic directly regulates FASN protein stability via post-translational modifications remains unclear. The present study reveals that O-GlcNAcylation at S509 stabilizes FASN by blocking its ubiquitin-proteasomal degradation. We propose that transcriptional priming (SREBP-1c) and post-translational stabilization (O-GlcNAcylation) act synergistically: the former initiates FASN expression, and the latter amplifies and maintains FASN protein levels under chronic arsenic exposure. This dual regulation ensures robust *de novo* lipogenesis in arsenic-induced MASLD.

Despite these findings, several questions remain regarding the broader implications of this axis. First, the full impact of FASN O-GlcNAcylation on lipid metabolism requires lipidomic analysis to assess changes in fatty acid composition and lipid class distribution. Moreover, although XBP1s is a transcriptional regulator of GFPT1, its broader target network involved in lipid metabolism and stress responses remains unexplored. RNA-seq and ChIP-seq would help identify additional XBP1s targets that may cooperate in promoting hepatic lipid accumulation. Future multiomics studies are needed to integrate this axis into the broader metabolic regulatory network.

In summary, on the basis of evidence from *in vivo* and *in vitro* models, the present study reveals the molecular mechanism through which arsenic exposure promotes MASLD progression. This work provides a theoretical foundation for targeting this mechanism, thereby guiding future efforts to validate it in human populations, identify biomarkers, and develop preventive measures.

■ ASSOCIATED CONTENT

Data Availability Statement

Data will be made available on request.

Supporting Information

The Supporting Information is available free of charge at https://pubs.acs.org/doi/10.1021/acs.jafc.6c00603.

Detailed materials and methods, primer sequences (Table S1), siRNA sequences (Table S2), antibodies (Table S3), and supporting results, including arsenic-induced hepatic phenotypes, transcriptional regulation, pathway valida-

https://doi.org/10.1021/acs.jafc.6c00603
J. Agric. Food Chem. XXXX, XXX, XXX−XXX

tion, site-specific mutation verification, and *in vivo* intervention studies (Figures S1−S9) (PDF)

AUTHOR INFORMATION

Corresponding Authors

Cheng Cheng − *Center for Global Health, China International Cooperation Center for Environment and Human Health, The Key Laboratory of Modern Toxicology, Ministry of Education, School of Public Health, Suzhou Institute for Advanced Study of Public Health, Gusu School, Nanjing Medical University, Nanjing 211166 Jiangsu, People's Republic of China*; Phone: +86-25-8686-8430; Email: drchengcheng@njmu.edu.cn

Qizhan Liu − *Center for Global Health, China International Cooperation Center for Environment and Human Health, The Key Laboratory of Modern Toxicology, Ministry of Education, School of Public Health, Suzhou Institute for Advanced Study of Public Health, Gusu School, Nanjing Medical University, Nanjing 211166 Jiangsu, People's Republic of China*; orcid.org/0000-0001-6107-9232; Phone: +86-25-8686-8424; Email: drqzliu@hotmail.com; Fax: +86-25 8686-8499

Authors

Wenjie Li − *Center for Global Health, China International Cooperation Center for Environment and Human Health, The Key Laboratory of Modern Toxicology, Ministry of Education, School of Public Health, Suzhou Institute for Advanced Study of Public Health, Gusu School, Nanjing Medical University, Nanjing 211166 Jiangsu, People's Republic of China*

Bowen Fan − *Center for Global Health, China International Cooperation Center for Environment and Human Health, The Key Laboratory of Modern Toxicology, Ministry of Education, School of Public Health, Suzhou Institute for Advanced Study of Public Health, Gusu School, Nanjing Medical University, Nanjing 211166 Jiangsu, People's Republic of China*

Han Li − *Dongguan Key Laboratory of Environmental Medicine, School of Public Health, Guangdong Medical University, Dongguan 523808 Guangdong, People's Republic of China*

Qiong Du − *Center for Global Health, China International Cooperation Center for Environment and Human Health, The Key Laboratory of Modern Toxicology, Ministry of Education, School of Public Health, Suzhou Institute for Advanced Study of Public Health, Gusu School, Nanjing Medical University, Nanjing 211166 Jiangsu, People's Republic of China*

Jiaheng Lin − *Center for Global Health, China International Cooperation Center for Environment and Human Health, The Key Laboratory of Modern Toxicology, Ministry of Education, School of Public Health, Suzhou Institute for Advanced Study of Public Health, Gusu School, Nanjing Medical University, Nanjing 211166 Jiangsu, People's Republic of China*

Yi Yang − *Center for Global Health, China International Cooperation Center for Environment and Human Health, The Key Laboratory of Modern Toxicology, Ministry of Education, School of Public Health, Suzhou Institute for Advanced Study of Public Health, Gusu School, Nanjing Medical University, Nanjing 211166 Jiangsu, People's Republic of China*; orcid.org/0000-0002-0045-215X

Xiaolin Ding − *Center for Global Health, China International Cooperation Center for Environment and Human Health, The Key Laboratory of Modern Toxicology, Ministry of Education, School of Public Health, Suzhou Institute for Advanced Study of Public Health, Gusu School, Nanjing Medical University, Nanjing 211166 Jiangsu, People's Republic of China*

Haoran Zhang − *Center for Global Health, China International Cooperation Center for Environment and Human Health, The Key Laboratory of Modern Toxicology, Ministry of Education, School of Public Health, Suzhou Institute for Advanced Study of Public Health, Gusu School, Nanjing Medical University, Nanjing 211166 Jiangsu, People's Republic of China*

Haibo Xia − *Center for Global Health, China International Cooperation Center for Environment and Human Health, The Key Laboratory of Modern Toxicology, Ministry of Education, School of Public Health, Suzhou Institute for Advanced Study of Public Health, Gusu School, Nanjing Medical University, Nanjing 211166 Jiangsu, People's Republic of China*

Binafsha Manzoor Syed − *Medical Research Center, Liaquat University of Medical & Health Sciences, Jamshoro 76090 Sindh, Pakistan*

Complete contact information is available at: https://pubs.acs.org/10.1021/acs.jafc.6c00603

Author Contributions

#W.L., B.F., H.L., and Q.D. contributed equally. Q.L., C.C., and W.L. developed the hypothesis. W.L., B.F., H.L., Q.D., J.L., X.D., and H.Z. performed the *vitro* experiments. W.L., B.F., H.L., Q.D., and Y.Y. conducted *vivo* experiments. C.C., H.X., and B.S. were responsible for the investigation and methodology. Q.L. and C.C. were responsible for the supervision and writing (review and editing). Q.L., H.L., and W.L. were responsible for funding acquisition.

Funding

This work was supported by the National Natural Science Foundations of China (82273660 and 81730089), the Priority Academic Program Development of Jiangsu Higher Education Institutions (2024), the Guangdong Medical Science and Technology Research Fund Project (A2025212), the Guangdong Basic and Applied Basic Research Foundation (2026A1515010796), and the 2024 Jiangsu Postgraduate Scientific Research Innovation Plan (SJCX24_0809).

Notes

The authors declare no competing financial interest.

ACKNOWLEDGMENTS

The authors thank Donald L. Hill (University of Alabama at Birmingham, USA), an experienced, English-speaking scientific editor for editing. The authors acknowledge the BioGDP (https://BioGDP.com), as schematics were constructed in the BioGDP platform.[67]

REFERENCES

(1) Podgorski, J.; Berg, M. Global threat of arsenic in groundwater. *Science (New York, N.Y.)* **2020**, *368* (6493), 845−850.

(2) Chen, Q. Y.; Costa, M. Arsenic: A Global Environmental Challenge. *Annual review of pharmacology and toxicology* **2021**, *61*, 47−63.

(3) Upadhyay, M. K.; Shukla, A.; Yadav, P.; Srivastava, S. A review of arsenic in crops, vegetables, animals and food products. *Food chemistry* **2019**, *276*, 608−618.

(4) Cai, Z.; Zhang, Y.; He, L.; Cui, M.; Zhang, W.; E, L.; Yang, H.; Ling, Q.; Hoffmann, P. R.; He, J.; Gou, S.; Liu, F.; Huang, Z. Methylseleninic Acid Elevating the Nrf2-GPX4 Axis Relieves

Endothelial Dysfunction and Ferroptosis Induced by Arsenic Exposure. *J. Agric. Food Chem.* **2025**, *73* (12), 7445−7455.
(5) Paul, S.; Giri, A. K. Epimutagenesis: A prospective mechanism to remediate arsenic-induced toxicity. *Environ. Int.* **2015**, *81*, 8−17.
(6) Shoaib, S. M.; Afzal, S.; Feezan, A.; Akash, M. S. H.; Nadeem, A.; Mir, T. M. Metabolomics Analysis and Biochemical Profiling of Arsenic-Induced Metabolic Impairment and Disease Susceptibility. *Biomolecules* **2023**, *13* (9), 1424.
(7) Hagström, H.; Shang, Y.; Hegmar, H.; Nasr, P. Natural history and progression of metabolic dysfunction-associated steatotic liver disease. *lancet. Gastroenterology & hepatology* **2024**, *9* (10), 944−956.
(8) Fan, B.; Cheng, C.; Yang, Y.; Wang, P.; Xia, H.; Wu, M.; Li, H.; Manzoor Syed, B.; Liu, Q. Construction of an adverse outcome pathway framework based on integrated data to evaluate arsenic-induced non-alcoholic fatty liver disease. *Environ. Int.* **2024**, *183*, No. 108381.
(9) Zhao, Y.; Guo, M.; Pei, T.; Shang, C.; Chen, Y.; Zhao, L.; Lu, Y.; Liang, C.; Wang, J.; Zhang, J. α-Lipoic Acid Ameliorates Arsenic-Induced Lipid Disorders by Promoting Peroxisomal β-Oxidation and Reducing Lipophagy in Chicken Hepatocyte. *Adv. Sci. (Weinheim, Ger.)* **2025**, *12* (11), No. e2413255.
(10) Wadgaonkar, P.; Chen, F. Connections between endoplasmic reticulum stress-associated unfolded protein response, mitochondria, and autophagy in arsenic-induced carcinogenesis. *Seminars in cancer biology* **2021**, *76*, 258−266.
(11) Renu, K.; Saravanan, A.; Elangovan, A.; Ramesh, S.; Annamalai, S.; Namachivayam, A.; Abel, P.; Madhyastha, H.; Madhyastha, R.; Maruyama, M.; Balachandar, V.; Valsala Gopalakrishnan, A. An appraisal on molecular and biochemical signalling cascades during arsenic-induced hepatotoxicity. *Life sciences* **2020**, *260*, No. 118438.
(12) Li, H.; Li, Z.; Chen, L.; Peng, X.; Wang, D.; Sun, Q.; Chen, Y.; Zhang, A.; Liu, Q.; Tang, H. PDHA1-mediated H3K18 lactylation is involved in arsenic-induced nonalcoholic fatty liver disease by activating the CD36-NLRP3 inflammasome axis. *Journal of hazardous materials* **2025**, *498*, No. 139852.
(13) Chen, W.; Wang, P.; Xie, Y.; Xie, D.; Wang, H.; Bu, N.; Lin, J.; Wu, M.; Xia, H.; Cheng, C.; Zhou, Y.; Liu, Q. Histone lactylation-augmented IRF4 is implicated in arsenite-induced liver fibrosis via modulating Th17 cell differentiation. *Chemico-biological interactions* **2025**, *414*, No. 111507.
(14) Dai, X.; Chen, C.; Yang, Q.; Xue, J.; Chen, X.; Sun, B.; Luo, F.; Liu, X.; Xiao, T.; Xu, H.; Sun, Q.; Zhang, A.; Liu, Q. Exosomal circRNA_100284 from arsenite-transformed cells, via microRNA-217 regulation of EZH2, is involved in the malignant transformation of human hepatic cells by accelerating the cell cycle and promoting cell proliferation. *Cell Death Dis.* **2018**, *9* (5), 454.
(15) Younossi, Z. M.; Kalligeros, M.; Henry, L. Epidemiology of metabolic dysfunction-associated steatotic liver disease. *Clin Mol. Hepatol* **2025**, *31* (Suppl), S32−s50.
(16) Chatham, J. C.; Zhang, J.; Wende, A. R. Role of O-Linked N-Acetylglucosamine Protein Modification in Cellular (Patho)-Physiology. *Physiol. Rev.* **2021**, *101* (2), 427−493.
(17) Moloughney, J. G.; Kim, P. K.; Vega-Cotto, N. M.; Wu, C. C.; Zhang, S.; Adlam, M.; Lynch, T.; Chou, P. C.; Rabinowitz, J. D.; Werlen, G.; Jacinto, E. mTORC2 Responds to Glutamine Catabolite Levels to Modulate the Hexosamine Biosynthesis Enzyme GFAT1. *Molecular cell* **2016**, *63* (5), 811−26.
(18) Saha, A.; Bello, D.; Fernández-Tejada, A. Advances in chemical probing of protein O-GlcNAc glycosylation: structural role and molecular mechanisms. *Chem. Soc. Rev.* **2021**, *50* (18), 10451−10485.
(19) Zhang, W.; Sun, Y.; Yang, Y.; Chen, Y. Impaired intracellular calcium homeostasis enhances protein O-GlcNAcylation and promotes vascular calcification and stiffness in diabetes. *Redox biology* **2023**, *63*, No. 102720.
(20) Lee, D. S.; An, T. H.; Kim, H.; Jung, E.; Kim, G.; Oh, S. Y.; Kim, J. S.; Chun, H. J.; Jung, J.; Lee, E. W.; Han, B. S.; Han, D. H.; Lee, Y. H.; Han, T. S.; Hur, K.; Lee, C. H.; Kim, D. S.; Kim, W. K.; Park, J. W.; Koo, S. H.; Seong, J. K.; Lee, S. C.; Kim, H.; Bae, K. H.; Oh, K. J. Tcf7l2 in hepatocytes regulates de novo lipogenesis in diet-induced non-alcoholic fatty liver disease in mice. *Diabetologia* **2023**, *66* (5), 931−954.
(21) Yang, F.; Chen, Y.; Zheng, G.; Gu, K.; Fan, L.; Li, T.; Zhu, L.; Yan, Y. LIMA1 O-GlcNAcylation Promotes Hepatic Lipid Deposition through Inducing β-catenin-Regulated FASn Expression in Metabolic Dysfunction-Associated Steatotic Liver Disease. *Adv. Sci. (Weinheim, Ger.)* **2025**, *12* (15), No. e2415941.
(22) Nóvoa, E.; da Silva Lima, N.; Gonzalez-Rellan, M. J.; Chantada-Vazquez, M. D. P.; Verheij, J.; Rodriguez, A.; Esquinas-Roman, E. M.; Fondevila, M. F.; Koning, M.; Fernandez, U.; Cabaleiro, A.; Parracho, T.; Iglesias-Moure, J.; Seoane, S.; Porteiro, B.; Escudero, A.; Senra, A.; Perez-Fernandez, R.; López, M.; Fidalgo, M.; Guallar, D.; Martinez-Chantar, M. L.; Dieguez, C.; Varela-Rey, M.; Prevot, V.; Schwaninger, M.; Meijnikman, A.; Bravo, S. B.; Frühbeck, G.; Nogueiras, R. Mitochondrial antiviral signaling protein enhances MASLD progression through the ERK/TNFα/NF$\kappa\beta$ pathway. *Hepatology (Baltimore, Md.)* **2025**, *81* (5), 1535−1552.
(23) Liu, S.; Zhang, X.; Yao, X.; Wang, G.; Huang, S.; Chen, P.; Tang, M.; Cai, J.; Wu, Z.; Zhang, Y.; Xu, R.; Liu, K.; He, K.; Wang, Y.; Jiang, L.; Wang, Q. A.; Rui, L.; Liu, J.; Liu, Y. Mammalian IRE1α dynamically and functionally coalesces with stress granules. *Nature cell biology* **2024**, *26* (6), 917−931.
(24) Zhu, C.; Xie, Y.; Li, Q.; Zhang, Z.; Chen, J.; Zhang, K.; Xia, X.; Yu, D.; Chen, D.; Yu, Z.; Chen, J. CPSF6-mediated XBP1 3′UTR shortening attenuates cisplatin-induced ER stress and elevates chemoresistance in lung adenocarcinoma. *Drug resistance updates: reviews and commentaries in antimicrobial and anticancer chemotherapy* **2023**, *68*, No. 100933.
(25) Cao, S.; Fachi, J. L.; Ma, K.; Ulezko Antonova, A.; Wang, Q.; Cai, Z.; Kaufman, R. J.; Ciorba, M. A.; Deepak, P.; Colonna, M. The IRE1α/XBP1 pathway sustains cytokine responses of group 3 innate lymphoid cells in inflammatory bowel disease. *J. Clin. Invest.* **2024**, *134* (13), No. e174198.
(26) Chen, L.; Bi, M.; Zhang, Z.; Du, X.; Chen, X.; Jiao, Q.; Jiang, H. The functions of IRE1α in neurodegenerative diseases: Beyond ER stress. *Ageing research reviews* **2022**, *82*, No. 101774.
(27) Wang, Q.; Zhou, H.; Bu, Q.; Wei, S.; Li, L.; Zhou, J.; Zhou, S.; Su, W.; Liu, M.; Liu, Z.; Wang, M.; Lu, L. Role of XBP1 in regulating the progression of non-alcoholic steatohepatitis. *Journal of hepatology* **2022**, *77* (2), 312−325.
(28) Tak, J.; Kim, Y. S.; Kim, S. G. Roles of X-box binding protein 1 in liver pathogenesis. *Clin Mol. Hepatol* **2025**, *31* (1), 1−31.
(29) Monteiro De Oliveira, E. C.; Caixeta, E. S.; Santos, V. S. V.; Pereira, B. B. Arsenic exposure from groundwater: environmental contamination, human health effects, and sustainable solutions. *Journal of toxicology and environmental health. Part B, Critical reviews* **2021**, *24* (3), 119−135.
(30) Li, H.; Wu, L.; Ye, F.; Wang, D.; Wang, L.; Li, W.; Xu, Y.; Li, Z.; Zhang, J.; Wang, S.; Zhang, A.; Liu, Q. As3MT via consuming SAM is involved in arsenic-induced nonalcoholic fatty liver disease by blocking m(6)A-mediated miR-142−5p maturation. *Science of the total environment* **2023**, *892*, No. 164746.
(31) Xiang, J.; Chen, C.; Liu, R.; Gou, D.; Chang, L.; Deng, H.; Gao, Q.; Zhang, W.; Tuo, L.; Pan, X.; Liang, L.; Xia, J.; Huang, L.; Yao, K.; Wang, B.; Hu, Z.; Huang, A.; Wang, K.; Tang, N. Gluconeogenic enzyme PCK1 deficiency promotes CHK2 O-GlcNAcylation and hepatocellular carcinoma growth upon glucose deprivation. *J. Clin. Invest.* **2021**, *131* (8), No. e144703.
(32) Du, H.; Li, J.; Wei, X.; Yang, D.; Zhang, B.; Fan, X.; Zhao, M.; Zhu, R.; Zhang, Z.; Zhang, Y.; Li, X.; Gu, N. Methylparaben induces hepatic glycolipid metabolism disorder by activating the IRE1α-XBP1 signaling pathway in male mice. *Environ. Int.* **2024**, *184*, No. 108445.
(33) Lane, E. A.; Choi, D. W.; Garcia-Haro, L.; Levine, Z. G.; Tedoldi, M.; Walker, S.; Danial, N. N. HCF-1 Regulates De Novo Lipogenesis through a Nutrient-Sensitive Complex with ChREBP. *Mol. Cell* **2019**, *75* (2), 357−371.
(34) Luo, X.; Alfason, L.; Wei, M.; Wu, S.; Kasim, V. Spliced or Unspliced, That Is the Question: The Biological Roles of XBP1 Isoforms in Pathophysiology. *Int. J. Mol. Sci.* **2022**, *23* (5), No. 2746.

https://doi.org/10.1021/acs.jafc.6c00603
J. Agric. Food Chem. XXXX, XXX, XXX−XXX

(35) Broutier, L.; Andersson-Rolf, A.; Hindley, C. J.; Boj, S. F.; Clevers, H.; Koo, B. K.; Huch, M. Culture and establishment of self-renewing human and mouse adult liver and pancreas 3D organoids and their genetic manipulation. *Nature protocols* **2016**, *11* (9), 1724−43.
(36) Targher, G.; Byrne, C. D.; Tilg, H. MASLD: a systemic metabolic disorder with cardiovascular and malignant complications. *Gut* **2024**, *73* (4), 691−702.
(37) Hagström, H.; Vessby, J.; Ekstedt, M.; Shang, Y. 99% of patients with NAFLD meet MASLD criteria and natural history is therefore identical. *Journal of hepatology* **2024**, *80* (2), e76−e77.
(38) Marmugi, A.; Ducheix, S.; Lasserre, F.; Polizzi, A.; Paris, A.; Priymenko, N.; Bertrand-Michel, J.; Pineau, T.; Guillou, H.; Martin, P. G.; Mselli-Lakhal, L. Low doses of bisphenol A induce gene expression related to lipid synthesis and trigger triglyceride accumulation in adult mouse liver. *Hepatology (Baltimore, Md.)* **2012**, *55* (2), 395−407.
(39) Gogola, T.; Pitkänen, S.; Huovinen, M.; Laitinen, H.; Küblbeck, J. Association between phthalate exposure and metabolic dysfunction-associated steatotic liver disease (MASLD) - Systematic literature review. *Environmental research* **2025**, *273*, No. 121186.
(40) Hu, Y.; He, W.; Huang, Y.; Xiang, H.; Guo, J.; Che, Y.; Cheng, X.; Hu, F.; Hu, M.; Ma, T.; Yu, J.; Tian, H.; Tian, S.; Ji, Y. X.; Zhang, P.; She, Z. G.; Zhang, X. J.; Huang, Z.; Yang, J.; Li, H. Fatty Acid Synthase-Suppressor Screening Identifies Sorting Nexin 8 as a Therapeutic Target for NAFLD. *Hepatology (Baltimore, Md.)* **2021**, *74* (5), 2508−2525.
(41) Zadra, G.; Ribeiro, C. F.; Chetta, P.; Ho, Y.; Cacciatore, S.; Gao, X.; Syamala, S.; Bango, C.; Photopoulos, C.; Huang, Y.; Tyekucheva, S.; Bastos, D. C.; Tchaicha, J.; Lawney, B.; Uo, T.; D'Anello, L.; Csibi, A.; Kalekar, R.; Larimer, B.; Ellis, L.; Butler, L. M.; Morrissey, C.; McGovern, K.; Palombella, V. J.; Kutok, J. L.; Mahmood, U.; Bosari, S.; Adams, J.; Peluso, S.; Dehm, S. M.; Plymate, S. R.; Loda, M. Inhibition of de novo lipogenesis targets androgen receptor signaling in castration-resistant prostate cancer. *Proc. Natl. Acad. Sci. U.S.A.* **2019**, *116* (2), 631−640.
(42) Wu, X.; Xu, M.; Geng, M.; Chen, S.; Little, P. J.; Xu, S.; Weng, J. Targeting protein modifications in metabolic diseases: molecular mechanisms and targeted therapies. *Signal Transduction Targeted Ther.* **2023**, *8* (1), 220.
(43) Zhang, L.; Han, C.; Shrestha, M. M.; Le, J.; Berger, W. K.; Huang, Y.; Desrouleaux, R.; Wang, E.; Nagy, L.; Yang, X. The OGT-TFF2 axis mediates intrahepatic crosstalk and MASH pathogenesis. *Hepatology (Baltimore, Md.)* **2025**, 10−1097.
(44) Zhang, W.; Zeng, S.; Huang, J.; Tian, X.; Wu, J.; Guo, L.; Liang, Y. Down-regulation of O-GlcNAcylation alleviates insulin signaling pathway impairment following arsenic exposure via suppressing the AMPK/mTOR-autophagy pathway. *Toxicology letters* **2024**, *397*, 67−78.
(45) Lam, C.; Low, J. Y.; Tran, P. T.; Wang, H. The hexosamine biosynthetic pathway and cancer: Current knowledge and future therapeutic strategies. *Cancer letters* **2021**, *503*, 11−18.
(46) Lei, Y.; Liu, Q.; Chen, B.; Wu, F.; Li, Y.; Dong, X.; Ma, N.; Wu, Z.; Zhu, Y.; Wang, L.; Fu, Y.; Liu, Y.; Song, Y.; Du, M.; Zhang, H.; Zhu, J.; Lyons, T. J.; Wang, T.; Hu, J.; Xu, H.; Chen, M.; Yan, H.; Wang, X. Protein O-GlcNAcylation coupled to Hippo signaling drives vascular dysfunction in diabetic retinopathy. *Nat. Commun.* **2024**, *15* (1), 9334.
(47) Yang, J. Y.; Zhang, R.; Zhang, Z. R.; Li, S.; Gong, D. A.; Li, C. H.; Chen, C.; Huang, L. Y.; Huang, A. L.; Tang, N.; Wang, K. GFAT1 promotes the progression of hepatocellular carcinoma via enhancing the O-GlcNAcylation of VEZF1. *Cell Death Dis.* **2025**, *16* (1), 647.
(48) Zhang, L.; Qi, B.; Li, Y.; Liang, X.; Zhang, Z.; Yang, T.; Jia, S.; Gao, X.; Chen, S.; Jiao, G.; Li, Y.; Zhou, H.; Chen, Y.; Li, Y.; Zhang, B.; Li, G.; Meng, C. GLUL mediates FOXO3 O-GlcNAcylation to regulate the osteogenic differentiation of BMSCs and senile osteoporosis. *Cell Death Differ.* **2025**, *32*, 2399−2411.
(49) Liu, Y.; Cao, Y.; Pan, X.; Shi, M.; Wu, Q.; Huang, T.; Jiang, H.; Li, W.; Zhang, J. O-GlcNAc elevation through activation of the hexosamine biosynthetic pathway enhances cancer cell chemoresistance. *Cell Death Dis.* **2018**, *9* (5), 485.
(50) Glembotski, C. C. Finding the missing link between the unfolded protein response and O-GlcNAcylation in the heart. *Circulation research* **2014**, *115* (6), 546−8.
(51) Wang, Z. V.; Deng, Y.; Gao, N.; Pedrozo, Z.; Li, D. L.; Morales, C. R.; Criollo, A.; Luo, X.; Tan, W.; Jiang, N.; Lehrman, M. A.; Rothermel, B. A.; Lee, A. H.; Lavandero, S.; Mammen, P. P. A.; Ferdous, A.; Gillette, T. G.; Scherer, P. E.; Hill, J. A. Spliced X-box binding protein 1 couples the unfolded protein response to hexosamine biosynthetic pathway. *Cell* **2014**, *156* (6), 1179−1192.
(52) Xu, X.; Liu, S.; Aodengqimuge; Wang, H.; Hu, M.; Xing, C.; Song, L. Arsenite Induces Vascular Endothelial Cell Dysfunction by Activating IRE1α/XBP1s/HIF1α-Dependent ANGII Signaling. *Toxicological sciences: an official journal of the Society of Toxicology* **2017**, *160* (2), 315−328.
(53) Zhang, W.; Zhao, E.; Li, Z.; Liu, W.; Wang, J.; Hou, W.; Zhang, N.; Yu, Y.; Li, X.; You, B. Hexokinase HK3-mediated O-GlcNAcylation of EP300: a key regulator of PD-L1 expression and immune evasion in ccRCC. *Cell Death Dis.* **2024**, *15* (8), 613.
(54) Zhou, X.; Wang, Y.; Li, X.; Zhou, J.; Yang, W.; Wang, X.; Jiao, S.; Zuo, W.; You, Z.; Ying, W.; Wu, C.; Bao, J. O-GlcNAcylation regulates the stability of transferrin receptor (TFRC) to control the ferroptosis in hepatocellular carcinoma cells. *Redox biology* **2024**, *73*, No. 103182.
(55) Zhu, H.; Zhao, T.; Zhao, S.; Yang, S.; Jiang, K.; Li, S.; Kang, Y.; Yang, Z.; Shen, J.; Shen, S.; Tao, H.; Xuan, J.; Yang, M.; Xu, B.; Wang, F.; Jiang, M. O-GlcNAcylation promotes the progression of non-alcoholic fatty liver disease by upregulating the expression and function of CD36. *Metabolism: clinical and experimental* **2024**, *156*, No. 155914.
(56) Zhu, Q.; Li, J.; Sun, H.; Fan, Z.; Hu, J.; Chai, S.; Lin, B.; Wu, L.; Qin, W.; Wang, Y.; Hsieh-Wilson, L. C.; Yi, W. O-GlcNAcylation of enolase 1 serves as a dual regulator of aerobic glycolysis and immune evasion in colorectal cancer. *Proc. Natl. Acad. Sci. U.S.A.* **2024**, *121* (44), No. e2408354121.
(57) Kang, D.; Lee, J.; Yook, G.; Jeong, S.; Shin, J.; Kim, M. S.; Kim, Y. J.; Jung, H.; Ahn, J.; Kim, T. W.; Chang, M. J.; Chang, C. B.; Kang, S. B.; Yang, W. H.; Lee, Y. H.; Cho, J. W.; Yi, E. C.; Kang, C.; Kim, J. H. Regulation of senescence-associated secretory phenotypes in osteoarthritis by cytosolic UDP-GlcNAc retention and O-GlcNAcylation. *Nat. Commun.* **2025**, *16* (1), 1094.
(58) Wu, H. Q.; Qin, R. C.; Li, W. J.; Liu, J. N.; Deng, C.; Zheng, Z. H.; Zheng, J. P.; Liu, Y.; Meng, Y. F.; Tang, C.; Tan, H. M.; Duan, F. F.; Tang, Y.; Xiao, F.; Lu, L. W.; Dai, X. Y.; Ma, K. Y. Inhibition of CDC27 O-GlcNAcylation coordinates the antitumor efficacy in multiple myeloma through the autophagy-lysosome pathway. *Acta pharmacologica Sinica* **2025**, *46* (7), 2041−2055.
(59) Herron, T. J.; Brüning-Richardson, A.; Gough, J. E.; Miller, A. F.; Pilkington, G. J.; Greenman, J.; Speirs, V.; Wu, J. C. Alternatives to animal testing are the future - it's time that journals, funders and scientists embrace them. *Nature* **2025**, *646* (8086), 799−801.
(60) Brooks, A.; Liang, X.; Zhang, Y.; Zhao, C. X.; Roberts, M. S.; Wang, H.; Zhang, L.; Crawford, D. H. G. Liver organoid as a 3D in vitro model for drug validation and toxicity assessment. *Pharmacological research* **2021**, *169*, No. 105608.
(61) Moon, J. H.; Roh, H. S.; Park, Y. J.; Song, H. H.; Choi, J.; Jung, D. W.; Park, S. J.; Park, H. J.; Park, S. H.; Kim, D. E.; Kim, G.; Auh, J. H.; Bhang, D. H.; Lee, H. J.; Lee, D. Y. A three-dimensional mouse liver organoid platform for assessing EDCs metabolites simulating liver metabolism. *Environ. Int.* **2025**, *195*, No. 109184.
(62) Ouyang, S.; Zhuo, S.; Yang, M.; Zhu, T.; Yu, S.; Li, Y.; Ying, H.; Le, Y. Glycerol Kinase Drives Hepatic de novo Lipogenesis and Triglyceride Synthesis in Nonalcoholic Fatty Liver by Activating SREBP-1c Transcription, Upregulating DGAT1/2 Expression, and Promoting Glycerol Metabolism. *Adv. Sci. (Weinheim, Ger.)* **2024**, *11* (46), No. e2401311.
(63) Li, Y.; Xu, S.; Mihaylova, M. M.; Zheng, B.; Hou, X.; Jiang, B.; Park, O.; Luo, Z.; Lefai, E.; Shyy, J. Y.; Gao, B.; Wierzbicki, M.; Verbeuren, T. J.; Shaw, R. J.; Cohen, R. A.; Zang, M. AMPK phosphorylates and inhibits SREBP activity to attenuate hepatic steatosis and atherosclerosis in diet-induced insulin-resistant mice. *Cell metabolism* **2011**, *13* (4), 376−388.

https://doi.org/10.1021/acs.jafc.6c00603
J. Agric. Food Chem. XXXX, XXX, XXX−XXX

(64) Ling, J.; Hua, L.; Qin, Y.; Gu, T.; Jiang, S.; Zhao, J. Perfluorooctane sulfonate promotes hepatic lipid accumulation and steatosis in high-fat diet mice through AMP-activated protein kinase/acetyl-CoA carboxylase (AMPK/ACC) pathway. *Journal of applied toxicology: JAT* **2023**, *43* (2), 312−322.
(65) Zhong, G.; Hu, T.; Tang, L.; Li, T.; Wu, S.; Duan, X.; Pan, J.; Zhang, H.; Tang, Z.; Feng, X.; Hu, L. Arsenic causes mitochondrial biogenesis obstacles by inhibiting the AMPK/PGC-1α signaling pathway and also induces apoptosis and dysregulated mitophagy in the duck liver. *Ecotoxicology and environmental safety* **2022**, *230*, No. 113117.
(66) Staels, B.; Butruille, L.; Francque, S. Treating NASH by targeting peroxisome proliferator-activated receptors. *Journal of hepatology* **2023**, *79* (5), 1302−1316.
(67) Jiang, S.; Li, H.; Zhang, L.; Mu, W.; Zhang, Y.; Chen, T.; Wu, J.; Tang, H.; Zheng, S.; Liu, Y.; Wu, Y.; Luo, X.; Xie, Y.; Ren, J. Generic Diagramming Platform (GDP): a comprehensive database of high-quality biomedical graphics. *Nucleic Acids Res.* **2025**, *53* (D1), D1670−D1676.

https://doi.org/10.1021/acs.jafc.6c00603
J. Agric. Food Chem. XXXX, XXX, XXX−XXX